Intracellular calcium carbonate biomineralization in *Cyanothece* sp. PCC 7425

Tove Jonsson

UPPSALA UNIVERSITET

UPTEC X 24049

Examensarbete 30 hp

June 2024

Intracellular Calcium Carbonate Biomineralization in *Cyanothece* sp. PCC 7425

Genetic Approaches to Uncover the Function of CcyA

Tove Jonsson

Civilingenjörsprogrammet i molekylär bioteknik

UPPSALA UNIVERSITET

Intracellular Calcium Carbonate Biomineralization in *Cyanothece* sp. PCC 7425 - Genetic Approaches to Uncover the Function of CcyA

Tove Jonsson

Abstract

Cyanobacteria are Gram-negative photosynthetic bacteria that historically have been linked to bacterial carbonate biomineralization, a process involving the precipitation of carbonate minerals made thermodynamically possible by metabolically active bacteria. The recent discovery of intracellular calcium carbonate formation in cyanobacteria has raised numerous questions about the mechanisms underlying cyanobacterial biomineralization. Traditionally believed to occur exclusively extracellularly, this process has now been observed intracellularly in specific cyanobacterial strains.

This project aimed to investigate the function of *ccyA*, a candidate marker gene for intracellular calcium carbonate formation (iACC), in *Cyanothece* sp. PCC 7425 through overexpression, deletion, and repression. The overexpression experiments of *ccyA* indicated a potential link between pH changes in growth media and Ca^{2+} uptake in *Cyanothece* sp. PCC 7425. While overexpression did not impact growth, it increased extracellular pH, usually an indicator for extracellular biomineralization. However, whether the changes in pH and Ca^{2+} uptake affected the formation of intracellular calcium carbonate granules remains to be investigated.

For deletion, the modern CRISPR/Cas12a system successfully deleted two *CAX* genes used as technical controls in *Cyanothece* sp. PCC 7425, establishing the system as a valid method for genomic modification. However, complete chromosome segregation of *ccyA* deletion was not achieved, indicating that *ccyA* might be crucial for *Cyanothece* sp. PCC 7425 survival. Partially segregated mutants obtained can still offer valuable information on *ccyA* and intracellular biomineralization in future experiments.

For repression, a CRISPR/dCas12a (CRISPRi) system was utilized. Experiments aimed at repressing *nblA*, a reporter gene, in *Cyanothece* sp. PCC 7425, did not produce a noticeable phenotype, likely due to physiological differences in *Cyanothece* sp. PCC 7425 as compared to model cyanobacteria used in previous research with *nblA* as a reporter. It could also be due to limitations in the inducibility of the CRISPRi system, with *Cyanothece* sp. PCC 7425 lacking the ability to import the inducer, IPTG.

Overall, this study provides a foundation for further exploration into the role of *ccyA* in intracellular biomineralization and offers insights into optimizing genetic tools for studying gene function in *Cyanothece* sp. PCC 7425.

Teknisk-naturvetenskapliga fakulteten Uppsala

universitet, Utgivningsort Uppsala

Handledare: Franck Chauvat Ämnesgranskare: Pia Lindberg

Examinator: Peter Kasson

Biomineralisering Inuti Cyanobakterier – Nyupptäckt Fenomen

Populärvetenskaplig sammanfattning

Tove Jonsson

Cyanobakterier, även kända som blågröna bakterier, är mest berömda för sin häpnadsväckande förmåga att fotosyntetisera. De omvandlar solljus och koldioxid till kemiskt lagrad energi och syret vi andas, och är därmed livsviktiga för vår överlevnad. En mindre allmänt känd egenskap för dessa blågröna bakterier är biomineralisering. När en cyanobakterie växer bildas biprodukter från deras metabolism vilket kan förändra kemiska faktorer, så som pH, vilket kan leda till att olika mineraler kan fällas ut, såsom kalciumkarbonat. Denna fällning har historiskt sett antagits ske endast utanför cellerna, men en ny upptäckt har visat att vissa cyanobakterier utnyttjar fällning inuti cellerna i form a granuler av kalciumkarbonat som även kan innehålla magnesium, barium, och strontium. Upptäckten av dessa granuler ifrågasätter vad man tidigare har trott om fysiologin hos dessa cyanobakterier och deras biomineralisering. Dessa granul-producerande cyanobakterier har även setts ha ett mycket större upptag av mineraler än de andra arterna. Dessutom har det påvisats att vissa arter kan inkorporera radioaktivt strontium och barium i sina granuler, vilket kan vara en framtida lösning för biosanering av radioaktivt avfall.

Forskning har hittat en gen som gemensamt finns i de granul-producerande cyanobakterierna och är frånvarande från övriga. Denna gen döptes till *ccyA* och i mitt projekt har jag undersökt om genen och dess protein CcyA är kopplat till denna intracellulära biomineraliseringsprocess och vilken funktion den kan ha. Detta arbete utfördes med granul-producerande cyanobakterien *Cyanothece* sp. PCC 7425 (C.7425), en organism som det finns begränsad kunskap om på grund av den begränsade forskningen som hittills genomförts. Arbetet resulterade i att lyckas implementera en modern metod för genmodifiering i C.7425 för att radera gener. Varpå resultatet från försök att radera *ccyA* pekar på att genen kan vara avgörande för organismens överlevnad, vilket kan betyda att produktionen av granuler också är det, om genen är direkt kopplad till processen. Ett annat experiment där *ccyA* från C.7425 och andra granul-producerande arter överuttrycktes i C.7425 visade samband mellan genen och viktiga parametrar för biomineralisering. Dessa samband innefattade ett högre upptag av kalcium och en ökning av pH utanför cellerna vilket tyder på CcyA kan vara en del av granul-produktionen.

Även om kopplingen mellan *ccyA* och den intracellulära biomineraliseringsprocessen samt CcyAs funktion fortfarande är odefinierade, har projektet lagt en grund för fortsatt forskning kring detta nyupptäckta spännande fenomen och vidare studier av C.7425.

Table of content

Abbreviations

aTc	Anhydrotetracycline
BG11	Blue green-11
CA	Carbonic anhydrase
$CaCO_3$	Calcium carbonate
CBBC	Calvin-Benson-Bassham cycle
CCM	CO_2 -concentrating mechanism
CcyA	Calcyanin
CEMOVIS	Cryo-electron microscopy of vitreous sections
Cm/Cm^S	Chloramphenicol/Chloramphenicol sensitive
CoBaHMA	Conserved basic residues in the heavy metal associated superfamily
CRISPR/Cas	Clustered regularly interspersed palindromic repeats/CRISPR-associated endonuclease
CRISPRi	CRISPR interference
crRNA	CRISPR-RNA
C.7425	*Cyanothece* sp. PCC 7425
DSB	Double stranded break
EPS	Extracellular polymeric substances
GlyZip	Glycine zipper
HCA	Hydrophobic cluster analysis
HCO_3^-	Bicarbonate
HDR	Homology directed repair
HMA	Heavy metal associated
iACC	Intracellular amorphous calcium carbonate
ICP-MS	Inductively coupled plasma - mass spectrometry
IMPMC	Institut de Minéralogie, Physique des Matériaux et Cosmochimie
Km/Km^R	Kanamycin/Kanamycin resistance
LB	Lysogeny broth
LBBC	Laboratoire de biologie et biotechnologie des Cyanobactéries
MM	Mineral media
Neo/Neo^R	Neomycin/Neomycin resistance
NHEJ	Non-homologous end joining
OD	Optical density
OriT	Origin of transfer
OriV	Origin of vegetative replication
PAM	Protospacer adjacent motif
PCC	Pasteur culture collection
PCR	Polymerase chain reaction
RT-PCR	Reverse transcription – polymerase chain reaction
RubisCO	Ribulose bi-phosphate carboxylase/oxygenase
SEM-EDXS	Scanning electron microscopy - energy dispersive x-ray
Sm/Sm^R	Streptomycin/Streptomycin resistance
Sp/Sp^R	Spectinomycin/Spectinomycin resistance
STEM-HAADF	Scanning transmission electron microscopy- high-angular annular dark field

1 Introduction

The recent discovery of intracellular calcium carbonate formation in cyanobacteria has given rise to a multitude of questions regarding cyanobacteria biomineralization (Benzerara *et al.* 2014; Couradeau *et al.* 2012; De Wever *et al.* 2019). What was previously believed to exclusively occur extracellularly has been found to happen intracellularly in certain strains. This project studied the formation of intracellular calcium carbonate granules using both traditional and newer genetic approaches with focus on the protein calcyanin (CcyA), predicted to have a significant association to this process.

1.1 Biomineralization in Cyanobacteria

Cyanobacteria are Gram-negative photosynthetic bacteria that colonise most environments on our planet. Their ability to capture carbon dioxide and produce di-oxygen makes this group integral to the planet's geochemical cycles (Görgen *et al.* 2020). Historically, cyanobacteria have been associated with bacterial carbonate biomineralization, which involves the precipitation of carbonate minerals rendered thermodynamically possible by metabolically active bacteria (Görgen *et al.* 2020). By modifying pH, metal activity and carbonate phases concentrations in the microenvironment, the saturation of a calcium solution can increase and exceed mineral solubility. Furthermore, organic polymers produced by the bacteria can also act as a preferential nucleation site, lowering the nucleation energy barrier for precipitation (Görgen *et al.* 2020). The bacterially induced storage and sequestration of atmospheric CO_2 to carbonate minerals by biomineralization makes it a widely studied research topic for carbon sink applications (Han *et al*. 2022; Lamérand *et al.* 2022; McCutcheon *et al.* 2019).

In the case of cyanobacteria's photosynthetic carbon fixation, uptake of both CO_2 and HCO_3^-, storage, and conversion of HCO_3^- to CO_2 is done by a complex set of molecular pathways known as CO_2-concentrating mechanisms (CCM), (Veaudor et al. 2020). The conversion of HCO_3^- to CO_2, the indirect substrate of the key carbon-fixing enzyme RubisCO (ribulose bi-phosphate carboxylase/oxygenase), is done by carbonic anhydrases (CA) in the O_2-free carboxysomes cell compartment, resulting in release of OH^- ions and an increase in CO_2 concentration around RubisCO (Veaudor et al. 2020). To uphold intracellular pH, OH^- are transported outside of the cell and H^+ are imported. It has been suggested that part of the H^+ import is performed by antiport of Ca^{2+} (Jiang *et al.* 2013). Together the increase in pH and carbonate phases extracellularly contributes to extracellular biomineralization (Couradeau *et al.* 2012 ; Görgen *et al.* 2020). See figure 1, for an overview of cyanobacterial extracellular biomineralization.

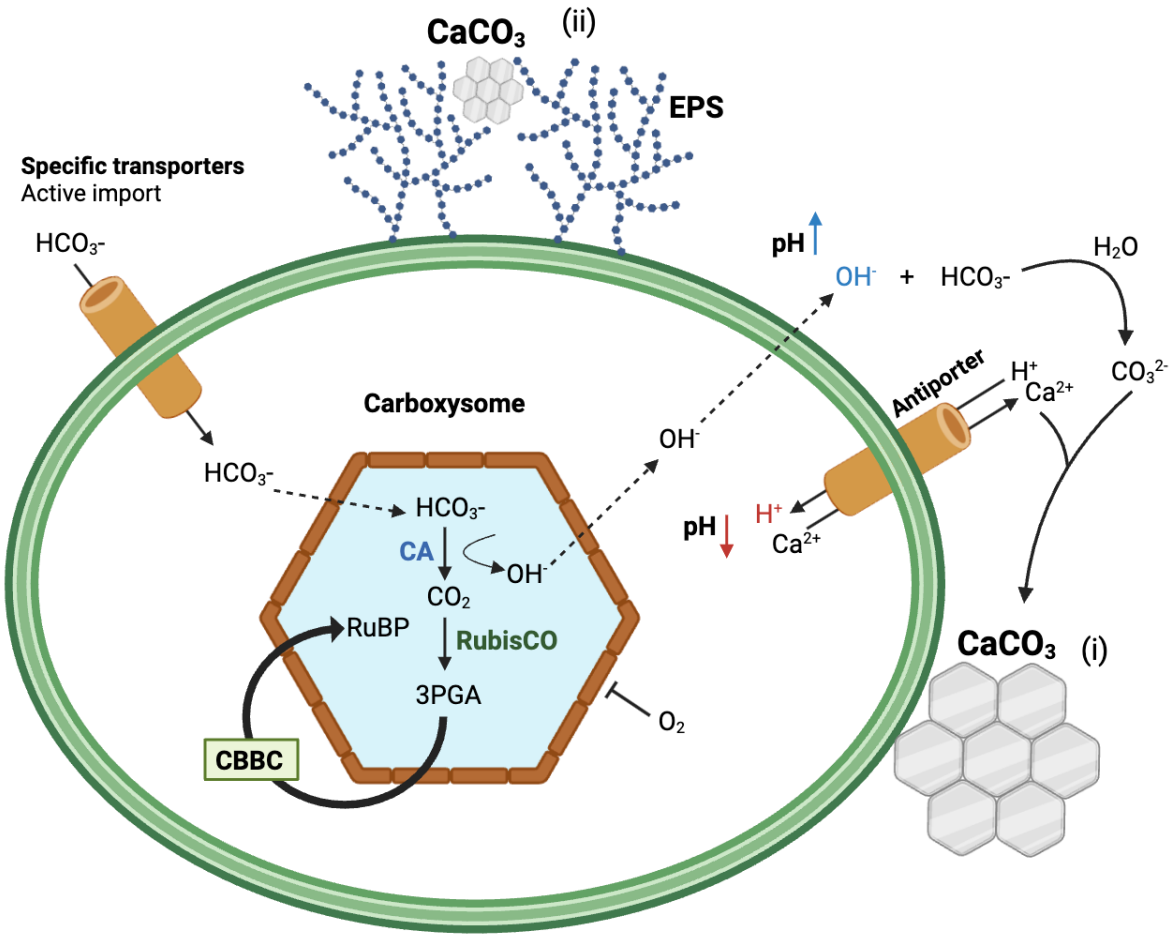

Figure 1: A simplified model of cyanobacterial extracellular biomineralization. (i) extracellular CaCO3 biomineralization as thought to be induced by CCM (Görgen et al 2020). It involves the uptake of HCO_3- where it is converted in the carboxysomes by carbonic anhydrases (CA) to CO_2 which releases OH^-. The CO_2 is fixed by RubisCO and used it the Calvin-Benson-Bassham cycle (CBBC). 3PGA; 3-phosphoglycerate; RuBP; ribulose-1,5-biphosphate. To buffer intracellular pH, H^+ is imported, in this example by a specific Ca^{2+}/H^+ antiporter (Jian et al. 2013). (ii) Extracellular polymeric substances (EPS) such as polysaccharides could act as preferential nucleation sites for $CaCO_3$ by local absorption of Ca^{2+} or decreased net interfacial energy between the solution and the growing $CaCO_3$ (Görgen et al. 2020). Both (i) and (ii) could occur for one cell simultaneously and connected.

1.2 Intracellular Amorphous Calcium Carbonate Formation

Historically, carbonate biomineralization was thought to occur only extracellularly. Recently however, it has been observed that certain cyanobacteria appear to be capable of intracellular amorphous calcium carbonate (iACC) biomineralization, generating intracellular $CaCO_3$ granules embedded in a microcompartment, suggesting a biologically controlled mineralization process (Benzerara *et al.* 2014; Blondeau *et al.* 2018; Couradeau *et al.* 2012; De Wever *et al.* 2019).

Couradeau *et al.* (2012) first identified this process in a cyanobacterium from modern microbialites in the highly alkaline lake Alchichica (Mexico) that contained intracellular amorphous Ca-Mg-Sr-Ba carbonate inclusions. Phylogenetic analyses placed it in a deep branching cyanobacteria order, and it was named *Gloeomargarita lithophora* (Moreira *et al.* 2017*)*. Benzerara *et al.* (2014), screened 68 strains of cyanobacteria, from the Pasteur Culture Collection (PCC) belonging to various genera, for iACC formations using SEM-EDXS (scanning electron microscopy - energy dispersive x-ray) analysis. They found eight diverse cyanobacteria species from geographically widespread and varied environments possessing amorphous calcium-rich inclusions differing in sizes and amounts. The localisation of the inclusions could follow two patterns depending on the strain. They can be seemingly scattered throughout the cytoplasm, as occurs in *G.lithophora* C7, or located at the cell poles and at cell septum prior to cell division, as observed in *Candidatus Synechococcus calcipolaris* G9 (Benzerara *et al.* 2014), see figure 2.

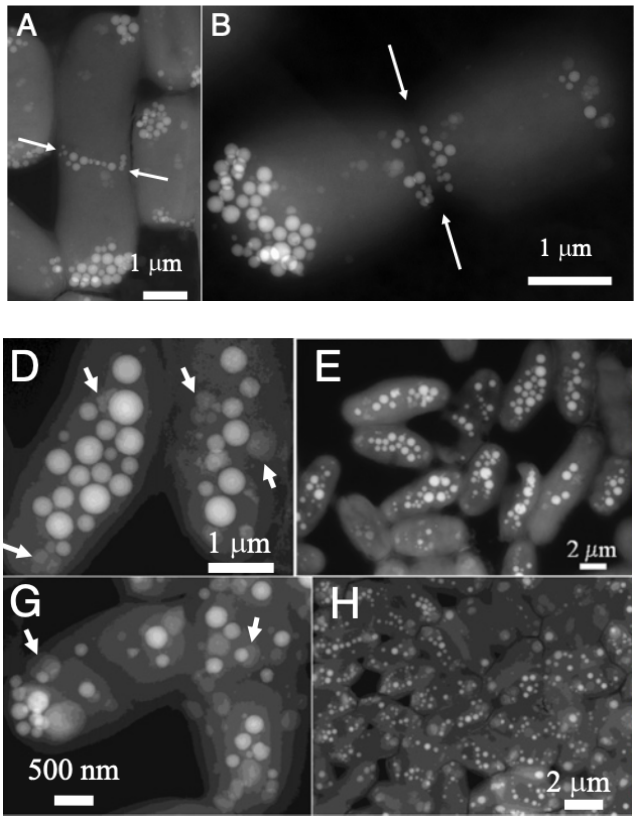

Figure 2: STEM-HAADF (scanning transmission electron microscopy- high-angular annular dark field) images of cyanobacteria forming intracellular carbonates granules localized at cell poles or scattered throughout the cells: (A and B) Synechococcus sp. PCC 6312, long and thin arrows show location were septation occurs. (D and E) Cyanothece sp. PCC 7425, arrows show poly-phosphate inclusions not iACC inclusions. (G and H) G. lithophora strain D10, arrows show same as for D. Figure from Benzerara et al. (2014).

Cyanobacterial cytoplasm is known to have a pH of ~6.8 – 7.9, high inorganic content of HCO_3^- at ~30 mM and an undersaturation of Ca^{2+} at ~100-200 nM, making Ca precipitation thermodynamically unfavourable (Blondeau *et al.* 2018). For formation of $CaCO_3$ granules, one or several of these cytoplasmic chemical parameters may differ, or there might be processes and/or subcellular compartments different from those of non-iACC-forming cyanobacteria. Cam *et al.* (2017) grew iACC-forming cyanobacteria in media undersaturated with respect to all Ca-carbonate phases and found that they still formed $CaCO_3$ granules. This indicates that iACC is an active cell process (likely costing energy) and therefore might be under genetic control. For example, nucleation and/or growth stages of the granules could involve specific pumps regulating ion concentrations intracellularly. It has also been proven that iACC-forming cyanobacteria have an increased Ca-sequestration ability (De Wever *et al.* 2019), suggesting that they require a higher amount of Ca^{2+} compared to non-iACC forming bacteria. Some strains forming iACC, such as *Cyanothece* sp. PCC 7425 and *G.lithophora* C7 have limited growth on media containing low Ca^{2+} concentration, 50 μM (De Wever *et al.* 2019). Cam *et al.* (2016), showed that *G.lithophora* has a selective and sequential sequestration of Ba, Sr and Ca even in the presence of high Ca^{2+} concentration. Normalising the uptake of Sr^{2+} and Br^{2+} by cell mass, *G.lithophora* had a greater uptake than most previously studied microorganisms (Cam *et al.* 2016). The capacity to produce Sr and Br carbonate inclusions, including ^{90}Sr radioactive strontium (Mehta *et al.* 2019), suggests that this intracellular biomineralization mechanism may have potential applications in the future for the bioremediation of nuclear plant effluents.

There are several hypotheses concerning the formation of the intracellular calcium carbonate granules. Blondeau *et al.* (2018), used CEMOVIS (cryo-electron microscopy of vitreous sections) to image ultrastructures of iACC-forming cyanobacteria. They found in all their strains that the inclusions were surrounded by a thin layer of ~2.5 nm, which is close to that of the carboxysome protein shell, ~2.9 to ~3.5 nm, and the lipid monolayer of thylakoids, ~1.9 to ~2.2 nm, in the same strains (Blondeau *et al*. 2018), see figure 3. They also concluded that the layer cannot be a lipid bilayer due to its appearance as a single electron dense line. The authors suggested that this intracellular microcompartment is allowing special chemical conditions, such as a high pH or saturation of Ca-carbonate phases favouring the formation of granules. To achieve precipitation inside the microcompartment calcium, carbonate and hydrogen transporters may be involved.

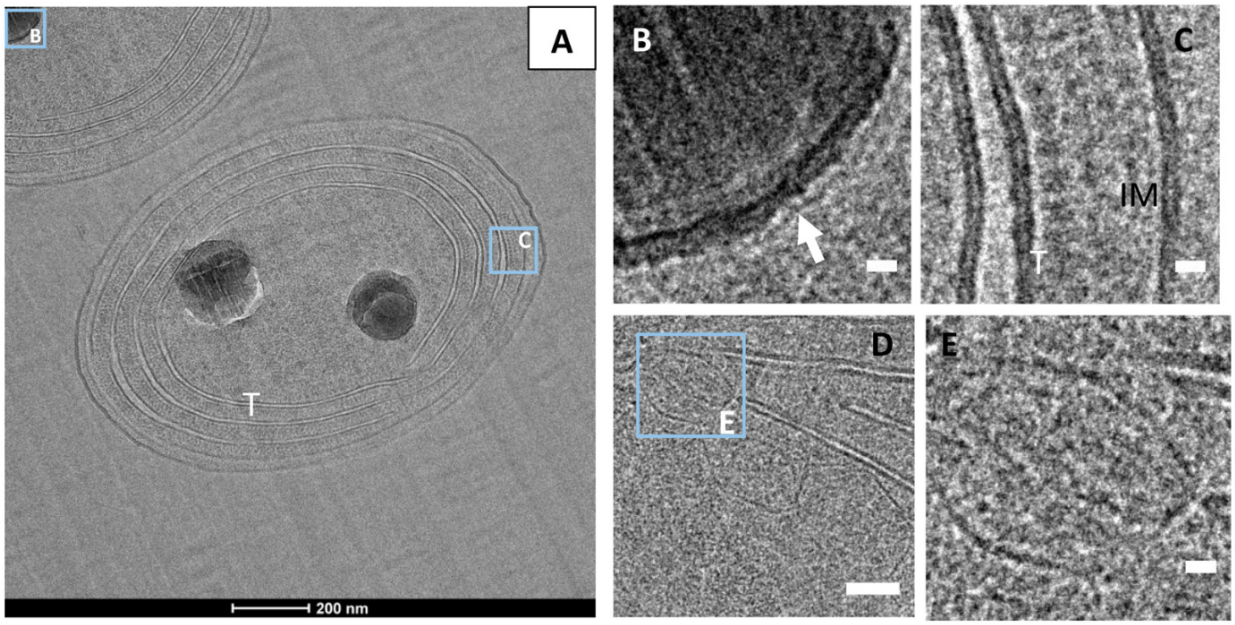

Figure 3: CEMOVIS images of ultrastructures in iACC-forming G.lithophora cells. (A) G. lithophora. (B) Close-up of $CaCO_3$-inclusion, arrow shows the thin layer that surrounds the inclusion (C) Close-up of lipid-bilayer of thylakoid (marked T) and cytoplasmic membranes (marked IM). (D) Carboxysome close to thylakoid. (E) Close-up of carboxysome protein shell. Scale bars: (B, C, E) 10 nm; D: 50 nm. Figure from Blondeau et al. (2018).

One hypothesis proposes that the granules are formed inside the carboxysomes. The local increase of carbonate phases and pH due to the CCM (Görgen *et al*. 2020), may favour such precipitation. Li *et al.* (2016) suggested the theory in the case of *G.lithophora* C7, as the typical number of carboxysomes, 2 to 6, per cell fell inside the range of inclusions per cell, 3-25. In this hypothesis, the larger number of inclusions could therefore be aborted carboxysomes. Another hypothesis from the same authors regarding, *S.calcipolaris* G9, suggests that the nucleation might somehow involve cell division proteins since the granules are located at mid-cell (septum) and cell poles where cyanobacteria cytokinetic proteins play important roles. It has been shown that in *E. coli*, the crucial cell division protein FtsZ, requires millimolar levels of Ca^{2+} for polymerization, which is preferential for the nucleation of Ca-carbonate (Li *et al.* 2016).

Why some cyanobacteria perform iACC formation is still unknown. Multiple possible physiological functions have been suggested. The inclusion may serve as ballasts for the cells, since they increase the density significantly, and therefore help adapt to benthic life (De Wever *et al.* 2019). Although, it seems unlikely to be the case for all iACC-forming strains as some are planktonic. The inclusions could also act as an intracellular pH regulation system and balance the OH^- formed from the CCM process or serve as an inorganic carbon reservoir for carbon-limited periods (De Wever *et al.* 2019). To learn about why they form the inclusions the genetic control, mechanism, and molecular properties of iACC formation needs to be identified.

1.3 *ccyA* – Candidate Marker Gene for Intracellular Biomineralization in Cyanobacteria

Previous studies described above hinted at the possibility of iACC formation being genetically controlled. By bioinformatic analyses, Benzerara *et al.* (2022) discovered a gene shared by iACC-forming cyanobacteria and absent from non-iACC forming strains. This orphan gene family and its predicted proteins were named *ccyA* and calcyanins, respectively. With the help of HCA (hydrophobic cluster analysis) calcyanins structure was divided into two domains (Benzerara *et al.* 2022), see figure 4. The conserved C-terminal harbours three repeats of a glycine zipper motif termed "GlyZip", which has a periodic pattern of three hydrophobic amino acids and one small, either glycine or alanine. This motif is common for helices in transmembrane proteins, especially homo-oligomeric proteins. Using the conserved C-terminal domain and sequenced cyanobacterial genomes available to search for homologs, Benzerara *et al.* (2022) found hits in additional cyanobacteria, whereupon out of 17 available for the study, 13 were detected to have iACC. This indicated that *ccyA* could be used as a diagnostic marker gene for intracellular biomineralization.

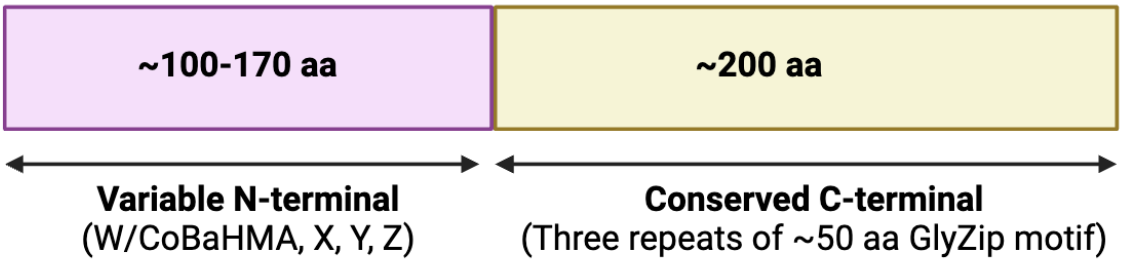

Figure 4: Schematic representation of Calcyanin showing its two protein domains: A variable N-terminal domain that can be categorised into four different types and a conserved C-terminal domain that possesses three repeats of the GlyZip motif.

The other calcyanin domain shows a variable N-terminal with hydrophobic clusters similar to secondary structures found in globular domains. The calcyanin homologs were categorised into four types based on their N-terminal domain W/CoBaHMA (Conserved Basic residues in the HMA (heavy metal associated) superfamily) , X, Y, and Z (Benzerara *et al.* 2022). The X- , Y- and Z-type N-terminal domains showed no significant similarity to known protein domains. On the other hand, the W/CoBaHMA-type domain showed significant similarity to heavy-metal associated (HMA) domains, commonly present in proteins involved in metal transport. The W/CoBaHMA-type domain also has a specific signature of basic residues, hence its name (Conserved Basic residues in the HMA superfamily). However, it does not have the two conserved cysteine residues involved in the binding of heavy metals, see figure 5 for comparison. To better understand the functional context of the CoBaHMA domain, Gaschignard *et al.* (2024) used AlphaFold2 to search for CoBaHMA domains in proteins different from calcyanin. They found it frequently linked to membrane proteins involved in

transport or lipid metabolism specific to bacteria. These proteins include P1B-type ATPases that transport metal cations as well as the P2A-ATPase family, including Ca^{2+} ATPases, a relevant finding in terms of calcium carbonate biomineralization.

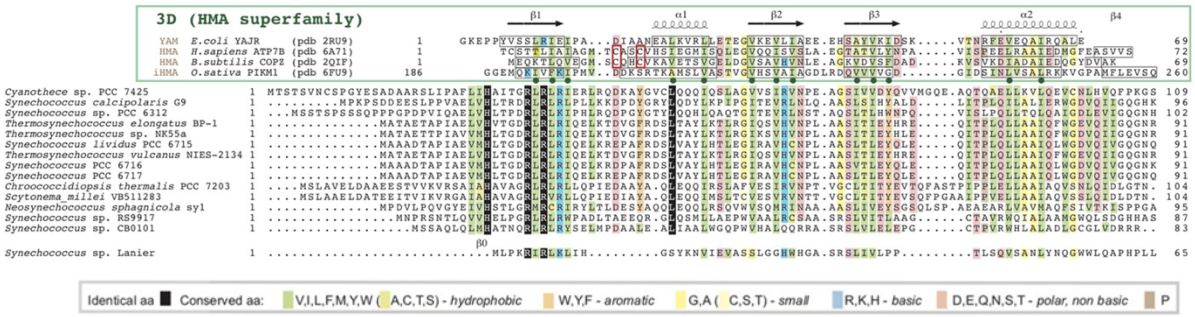

Figure 5: Multiple sequence alignment of several calcyanin CoBaHMA domain from cyanobacteria to HMA superfamily members. Similar amino acids are colour coded according to their properties, the two cysteines involved in metal binding are boxed in red, and identical conserved amino acids are coloured black. The HMA superfamily members have their known 3D structures showcased on top and the calcyanin CoBaHMA domain showcases an additional predicted β-strand on the bottom.

Based on the compartmentalization of the iACC inclusions, calcyanin could act in the transport of carbonate phases such as HCO_3- or the alkaline earth elements Ca^{2+}, Mg^{2+}, Sr^{2+} and Ba^{2+}, either at membrane level or at inclusion level. Calcyanin could also serve as a nucleation site for precipitation or be involved in the regulation and signalling for iACC formation.

1.4 Analysis of the *ccyA* Gene in iACC-forming Cyanobacteria

Numerous indications suggest that *ccyA* is directly or indirectly involved in the iACC formation, with its protein product calcyanin, showing structural attributes related to compartmentalization and regulation. Therefore, genetic methods described below were deployed to study the function of *ccyA* in iACC-formation.

1.4.1 *Cyanothece* sp. PCC 7425 - An Interesting Reporter Strain for the Analysis of iACC and the *ccyA* Gene

The cyanobacteria capable of intracellular biomineralization are evolutionary distant and often poorly studied. To study the role of *ccyA* on iACC formation, *Cyanothece* sp. PCC 7425 (hereafter C.7425) was selected for the following reasons.

Cyanothece is a genus of morphologically diverse and unicellular diazotrophic cyanobacteria (Bandyopadhyay *et al.* 2011). C.7425 have large cells, about 3-4 µm, which is beneficial for analysis of intracellular localization of iACC granules (Benzerara *et al*. 2014), as well as proteins and subcellular structures (Chenebault et al. 2020). C.7425 grows well in both liquid and solid media under standard photoautotrophic conditions (35 µE and 30°C), with a doubling time of 24 hours (Chenebault *et al.* 2020) *i.e.* 7-fold faster than *G. lithophora*. C.7425 also has a robust circadian rhythm (Bandyopadhyay *et al.* 2011). Appreciatively, C.7425 is able to propagate autonomously replicating plasmids derived from the broad-host-range plasmid RSF1010, extensively used for genetic analysis in model strains such as *Synechocystis* PCC 6803 and *Synechococcus* PCC 7942 (Cassier-Chauvat et al. 2021) and further described in the chapter below. These vectors are useful tools for high-level gene expression and analysis of subcellular localization of proteins, using common antibiotics for selection such as Kanamycin (Km), Streptomycin (Sm), and Spectinomycin (Sp) (Chenebault *et al.* 2020). Furthermore, the calcium carbonate inclusions in C.7425 are sizable, ranging from 130 to 700 nm, and dispersed throughout the cytoplasm, typically occurring in quantities of 2 to 20 per cell (Benzerara *et al.* 2014), which simplifies verification via SEM. Additionally, C.7425 harbours the *ccyA* sequence containing the interesting W/CoBaHMA-type calcyanin (Benzerara *et al.* 2022).

1.4.2 Genetic Analysis of *ccyA* in *Cyanothece* sp. PCC 7425

To study the role of *ccyA* on the intracellular biomineralization in C.7425 both traditional and newer genetic engineering strategies were deployed in this project. Broad-host-range plasmids can sustain themselves in a variety of bacterial species (Jain & Srivastava 2013). RSF1010, for example, carries genes such as repA, repB, and repC, which enable autonomous replication (Jain & Srivastava 2013). The RSF1010 can therefore replicate in a wide range of Gram-negative bacteria, including *E. coli* and evolutionary-diverse cyanobacteria genera such as C.7425 (Chenebault *et al.* 2020), without containing a cyanobacterial replicon (Cassier-Chauvat *et al.* 2021). Derivative of broad-host-range plasmids for studying genes of interest are generated in *E. coli* using standard molecular biology techniques and then transferred to cyanobacterial hosts for testing gene function.

Some cyanobacterial strains are naturally transformable, readily taking up exogenous DNA at the right physiological conditions (Cassier-Chauvat *et al.* 2021). For strains that lack natural transformation capabilities, conjugation is a widely used method, notably the most efficient method for introducing RSF1010 and its derivatives (Cassier-Chauvat *et al.* 2021), with instances where it can be even more efficient than natural transformation for strains that are naturally transformable (Vavitsas *et al.* 2021). In this project, a triparental conjugation method is utilised for introduction of all RSF1010-derived plasmids into their respective cyanobacteria. For this method, the plasmid of interest (in this project RSF1010 derivatives), is constructed using an *E. coli* strain dedicated to gene cloning which is subsequently co-incubated together with an *E. coli* helper strain and the recipient cyanobacteria (Cassier-Chauvat *et al.* 2021; Chenebault *et al.* 2020). The helper strain houses the conjugative, self-transferable plasmid RP4 that does not replicate in cyanobacteria but encodes genes necessary for the transfer of the nonself-transmissible, but mobilizable, broad-host-range vector to the recipient cyanobacterium (Cassier-Chauvat *et al.* 2021). For an overview of the principle of triparental conjugation, see figure 6.

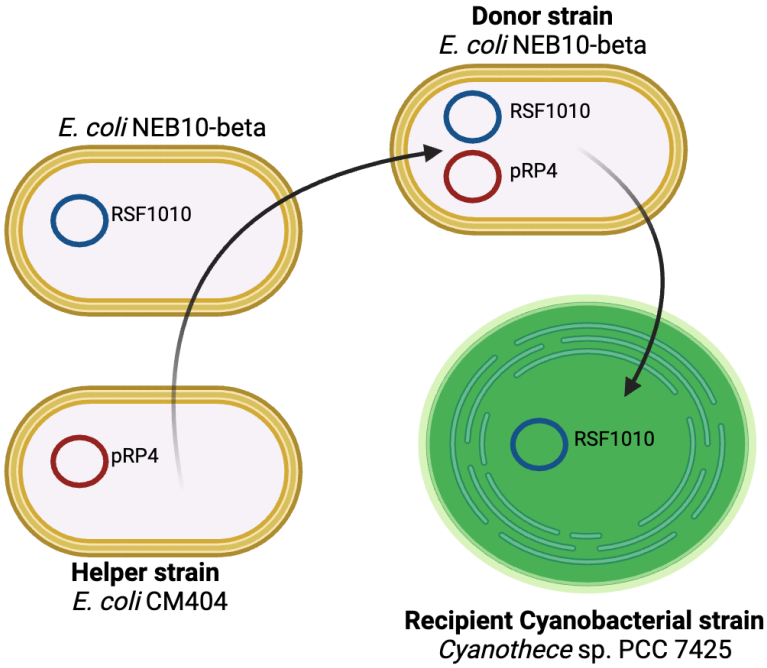

Figure 6: Triparental conjugation of RSF1010 into a cyanobacterial strain, such as C.7425. Helper strain E. coli CM404 housing the self-transferable plasmid RP4 "pRP4", E. coli NEB10-beta housing the mobilizable RSF1010-derived cloning vector and the recipient cyanobacteria are incubated together. Through cell to cell contact RP4 is self- transferred into the donor strain, where it can help transfer the RSF1010 vector into the recipient cyanobacteria where it replicates unlike RP4.

The aim of this project was to characterize the formation of iACC formation in C.7425 by studying *ccyA*. As mentioned above, to investigate the effect, overexpression, deletion, and inactivation of *ccyA* was employed.

For overexpression in C.7425, the RSF1010-derived pC vector was used, which possesses the strong λ phage *pR* promoter for constitutive expression (Mermet-Bouvier & Chauvat 1994). Upon cloning a *ccyA* gene into the pC-plasmid using the restrictions sites NdeI and EcoRI, the *E. coli* transformants will be streptomycin (Sm^R) and spectinomycin (Sp^R) resistant and chloramphenicol sensitive (Cm^S), see figure 7. Three pC plasmids were constructed, previous to this project (Unpublished data, Görgen), housing the respective *ccyA* sequence from *Synechococcus* sp. PCC 6312, *Gloeomargarita lithphora* C7, and C.7425, see Appendix B for list. The *ccyA* genes chosen come from cyanobacteria that exhibit different localization of inclusions and/or have different N-terminal domain of calcyanin, see table 1. Important to keep in mind, that it is not yet known if *ccyA* acts in the formation of the granules, therefore they might not be related to the differences in localization of the inclusions.

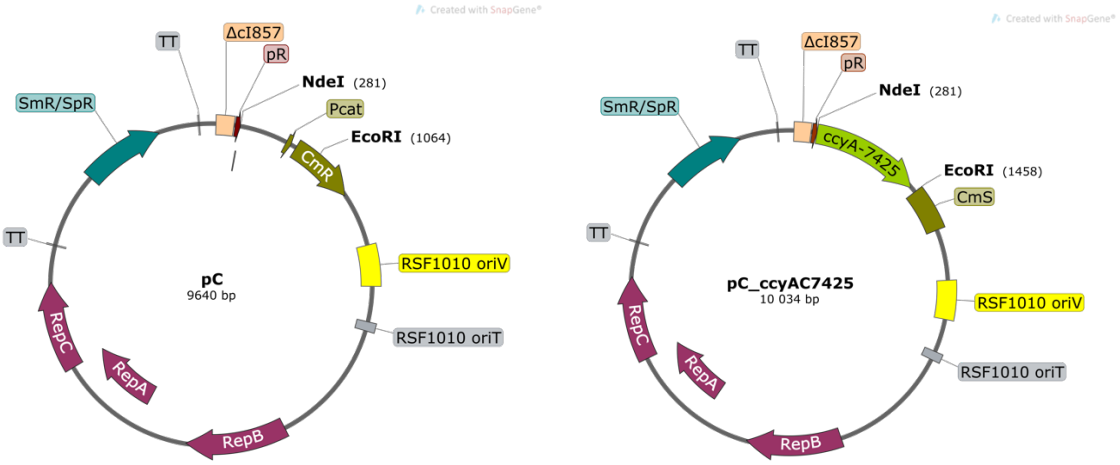

Figure 7: Left: pC plasmid containing; strong λ phage promoter "pR", Sm^R/Sp^R selectable marker "SmR/SpR", the chloramphenicol resistance gene "CmR" expressed from its own promoter "Pcat", restriction sites "NdeI" and EcoRI", and the RSF1010 replication genes repA, repB, and repC. ΔcI857 is a truncated repressor gene to no longer control pR activity by growth temperature (Mermet-Bouvier & Chauvat 1994), hence pR activity is strong and constitutive. Right: pC plasmid with ccyA from C.7425 inserted between NdeI and EcoRI, resulting in truncated CmR and therefore shows chloramphenicol sensitivity "CmS". RSF1010 oriT (origin of transfer) and oriV (origin of vegetative replication) are needed for transfer (oriT) and replication (oriV) into recipient cyanobacteria.

Table 1: List of ccyA genes that were inserted into their respective pC-plasmid and transferred via triparental conjugation into respective C.7425 cultures for overexpression experiment.

***Origin of ccyA* genes**	**Calcyanin N-terminal domain type**	**Granules localization in native strain**
Synechococcus sp. PCC 6312	W/CoBaHMA	Clustered at cell poles
Gloeomargarita lithphora C7	X	Scattered throughout the cytoplasm
Cyanothece sp. PCC 7425	W/CoBaHMA	Scattered throughout the cytoplasm

However, to test if *ccyA* acts in the iACC process, deletion or repression of *ccyA* is paramount. Deletion, in cyanobacteria is often a time-consuming process, as compared to some prokaryotes (Cassier-Chauvat *et al.* 2021; Vavitsas *et al.* 2021). This is due to the slower growth times and polyploidy of cyanobacteria. They possess multiple copies of their chromosome per cell, resulting in the need of complete chromosome segregation for a deletion to be fully effective and stable over time (Cassier-Chauvat *et al.* 2021). To speed up the process, newer technologies of multiplexed engineering and silencing are on the rise, such as markerless CRISPR-based editing (Vavitsas *et al.* 2021).

CRISPR/Cas (clustered regularly interspersed palindromic repeats/CRISPR-associated endonuclease) systems are adaptive immune systems universally found in archaea and bacteria (Niu *et al.* 2019). These systems have been developed for efficient bioengineering in a multitude of organisms, spanning both prokaryotes and eukaryotes. The Cas-effector protein is an RNA-guided endonuclease that can be directed by a site-specific RNA sequence (crRNA) to induce double stranded break (DSB) on DNA (Cassier-Chauvat *et al.* 2021; Niu *et al.* 2019). Cells have the ability to repair the DNA break by non-homologous end joining (NHEJ), which can cause random insertions or deletions, or homology-directed repair (HDR), resulting in an insert of a chosen sequence from a supplied homologous repair template (Niu *et al.* 2019). The crRNA consists of a spacer sequence complementary to the target DNA site (protospacer) and is matured from a pre-crRNA array (CRISPR array) of spacer sequences with palindromic repeats in between (Niu *et al.* 2019). Most CRISPR/Cas systems also require a protospacer adjacent motif (PAM) recognized by the nuclease next to the target site. The first system developed for genetic manipulation is the CRISPR/Cas9 (Niu *et al.* 2019), which can be toxic to cyanobacteria to varying degree depending on the tested strain and level of expression (Niu *et al.* 2019; Ungerer & Pakrasi 2016; Wendt *et al.* 2016). To circumvent this problem, the Cas12a (formerly known as Cpf1) nuclease was tested instead and showed efficient genome editing in several cyanobacteria strains (Niu *et al.* 2019; Ungerer & Pakrasi 2016). Cas12a has some advantages compared to Cas9. Cas9 produces a blunt DSB directly next to its PAM motif, which can cause a disruption to the protospacer sequence if the organism undergoes NHEJ to repair the break (Ungerer & Pakrasi 2016). While Cas12a makes a staggered cut 17 bp away from the PAM, leaving it undisrupted in case of NHEJ and can therefore cut again until desired HDR (Ungerer & Pakrasi 2016). Cas12a requires only the nuclease and the CRISPR array, unlike Cas9 that needs tracrRNA for maturing crRNA and for DNA cleavage, significantly simplifying the system (Ungerer & Pakrasi 2016). For the above reasons, in this project the CIRSPR/Cas12a system was chosen for genetic manipulation of *ccyA*.

The CRISPR/Cas12a constructs in this project were made from the RSF1010-derived pSL2680 vector created by Himadri Pakrasi Lab (Ungerer & Pakrasi 2016). The base plasmid houses the Cas12a gene with a fused *E. coli lac* promoter. It also contains a *LacZα* with a *lac* operator and promoter adjoined by two *Aar*I restriction sites, whereupon the spacers for the CRISPR array can be inserted to make the editing plasmid. When cloned with the editing plasmid, the *E. coli* transformants will be kanamycin (Km^R)/neomycin (Neo^R) resistant and susceptible to blue-white screening due to *LacZα* exchange with the spacer inserts. For HDR, pSL2680 contains a *Sal*I restriction site for insertion of a homologous repair template. Upstream of both the CRISPR array and the homology repair template is a J23119 constitutive promoter for expression. For an overview of the base plasmid and the editing plasmid with insert for deletion and HDR of *ccyA* in C.7425, see figure 8.

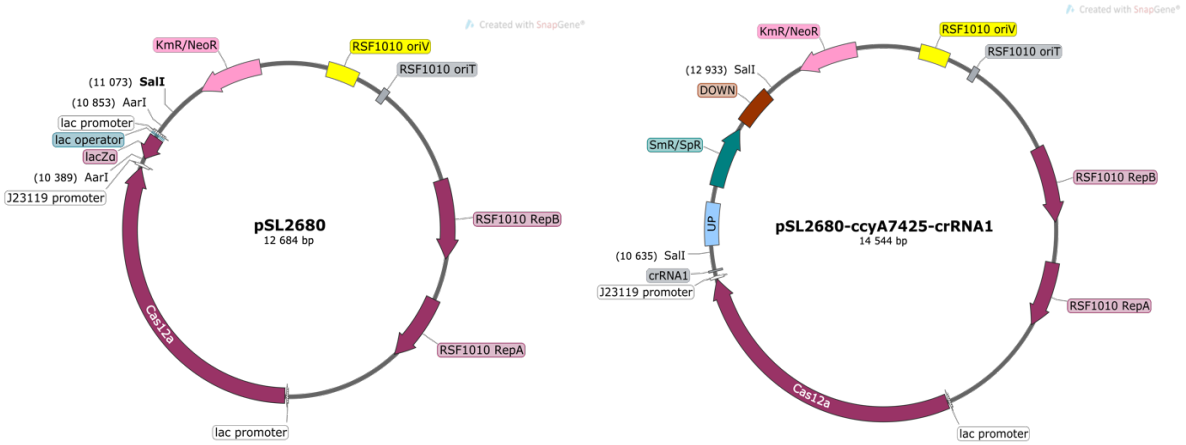

Figure 8: Left: RSF1010 derived pSL2680 base plasmid containing; Cas12a gene with lac promoter, LacZα with lac operator and promoter, Km^R/Neo^R selectable marker "KmR/NeoR", two AarI restriction sites for insertion of spacers, one SalI restriction site for insertion of homology repair template, and a J23119 strong constitutive promoter for expression of two previous mentioned insertions. Right: pSL2680 editing plasmid with insertion of a single spacer for ccyA to make the CRISPR array ,"crRNA1", and insertion of homology repair template containing upstream ("UP"), downstream ("DOWN") regions of the ccyA on C.7425 chromosome and a Sm^R/Sp^R selectable marker "SmR/SpR". Transformants will therefore be Sm^R, Sp^R, Km^R and Neo^R.

Previous work using pSL2680 derived editing plasmids to delete *ccyA* and glutathione reductase gene in C.7425 have been done at my host lab Laboratoire de biologie et biotechnologie des Cyanobactéries (LBBC), and resulted in successful KO mutant of glutathione reductase but not of *ccyA* (unpublished data, LBBC). Therefore, as a technical control, two predicted Ca^{2+}/H^+ antiporter genes (De Wever *et al.* 2019), were also targeted in C.7425. In this project they are referred to as *CAX3000* and *CAX3001* and were aimed to be deleted with one HDR, using a homology repair template spanning both genes. In total, there are four predicted Ca^{2+}/H^+ antiporter genes in C.7425 (De Wever *et al.* 2019). The *CAX* genes were also chosen based on the premise that a successful deletion would simultaneously delete two out of four *CAX* genes, increasing the odds of generating interesting C.7425 mutant for future intracellular biomineralization analysis. For an overview of each targeted deletion in C.7425, see figure 9.

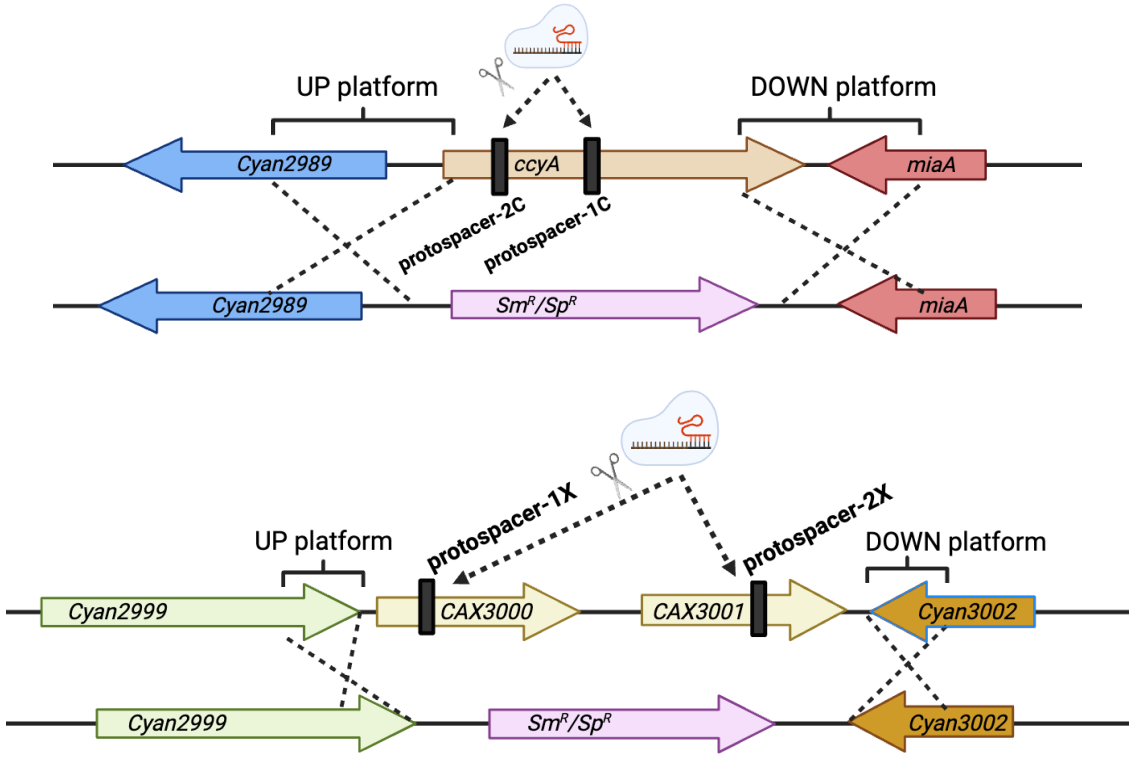

Figure 9: Schematic representation of protospacers on the chromosome of C.7425 to which the Cas12a is guided to perform a DSB whereafter HDR can occur using UP and DOWN platforms resulting in insertion of an Sm^R/Sp^R cassette on the chromosome. Dotted lines represent homologous recombination. Dotted lines with small black arrows represent to where the Cas12a is guided. Top: deletion of ccyA.gene on C.7425 chromosome. Bottom: deletion of the CAX3000 and CAX3001 genes on C.7425 chromosome.

If *ccyA* is crucial to C.7425 life, it will be difficult to delete from all chromosome copies, such cells will die. In this case, a variant of the CRISPR/Cas system can be used, namely CRISPRi (CRISPR interference). This related technology utilises a mutant deactivated nuclease, unable to cut DNA, which instead just binds to the specific site and thereby sterically hindering RNA polymerase from transcribing the studied gene, hence decreasing (fully or partially) its expression (Knoot *et al.* 2019). The possibility of multiplexing repression of essential genes, makes CRISPRi systems attractive for biotechnological applications to increase product titres (Knoot *et al.* 2019). Since expression of the dCas nucleases can be toxic to cyanobacteria, the CRISPRi systems, dCas12a and the CRISPR array, are often put under tight repression using inducible systems for expression (Knoot *et al.* 2019). For this project, a deactivated Cas12a (dCas12a) was chosen for the goal of repressing *ccyA* in C.7425.

The CRISPRi constructs were made from the pSL3287 vector created by Himadri Pakrasi Lab (Knoot *et al.* 2019). The base vector pSL3287 contains the deactivated Cas12a, dCas12a gene under control of a *trc* promotor adjoined by two symmetric lac operator sequences, *trc*2O, for titratable induction with IPTG (isopropyl ß-D-1-thiogalactopyranoside). Knoot *et al*. (2019) reminded that previous research showed that tying expression of the Cas-effector protein and the CRISPR array to the same inducer resulted in the largest repression range. Therefore, the CRISPR array in pSL3287 derived vectors are under control of an *E. coli lac* promotor with one symmetric lac operator, *lac*1O. For repression of the promotors, the vector contains the enhanced *lacI* repressor mutant W220F, "lacImut", under control of the J23119 promotor for constitutive expression. The spacers for the CRISPR array can be inserted at *Aar*I restrictions sites, whereupon successful insertion a *LacZα,* with its *lac* promotor and operator, is removed. pSL3287 also has an RSF1010-type mobilization and replicon region for conjugation and autonomous replication. When cloned with a pSL3287 with inserted spacers, transformants will be Km^R and susceptible to blue-white screening, see figure 10.

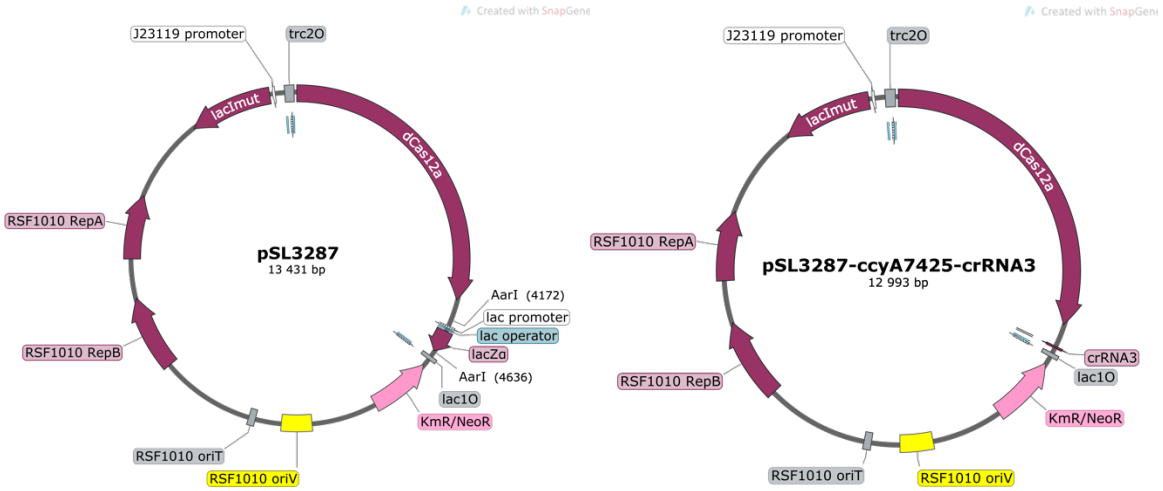

Figure 10: Left: pSL3287 base plasmid containing: dCas12a gene under control of IPTG-inducible system "trc2O", LacZα with lac operator and promotor, two AarI restriction sites for future insertion of a CRISPR array, "lac1O" IPTG-inducible system for future expression of CRISPR array, a lacI repressor mutant "lacImut" under control of constitutive J23119 promotor, and a Km^R/Neo^R selection marker "KmR/NeoR". Right: pSL3287 with insertion of a single spacer in the CRISPR array "crRNA3" for inactivation of ccyA in C.7425.

Apart from repression of *ccyA*, two genes predicted to encode for the phycobilisome degradation protein NblA, *nblA2827* and *nblA0220*, were also targeted as technical controls as it is known to produce an easily observable phenotype in cyanobacteria (Baldanta *et al.* 2022). Phybocbilisomes are large light harvesting antenna protein complexes that can reach 4 MDa in size (Sendersky *et al*. 2015). During nitrogen deficiency, transcription of *nblA* increases for degradation of the phycobilisomes to serve as a temporary nitrogen source for cell survival (Sendersky *et al.* 2015; Sun Young Choi & Han Min Woo 2020). As a result, the culture will turn from normal blue-green colour (normal abundance of phycobilisomes) to yellow (low content/absence of phycobilisomes). Therefore, repression of *nblA* using CRISPRi should produce a null phenotype that stays blue-green during nitrogen starvation as observed in model cyanobacteria (Baldanta *et al.* 2022; Sun Young Choi & Han Min Woo 2020). This phenotypic change of colour can be easily distinguished visually and therefore should hint at the success of the CRISPRi system in C.7425 without the need to analyse transcription levels (Sun Young Choi & Han Min Woo 2020). For an overview of each targeted gene repression in C.7425, see figure 11. In this project, pSL3287 constructs were also made with CRISPR arrays containing two spacers for targeted repression, see Appendix B for a list. This means that a successful CRISPRi system would produce a mix of dCas12a nucleases with crRNAs containing respective spacers. For example, regarding *nblA* repression, both *nblA* genes would be repressed simultaneously in one cell.

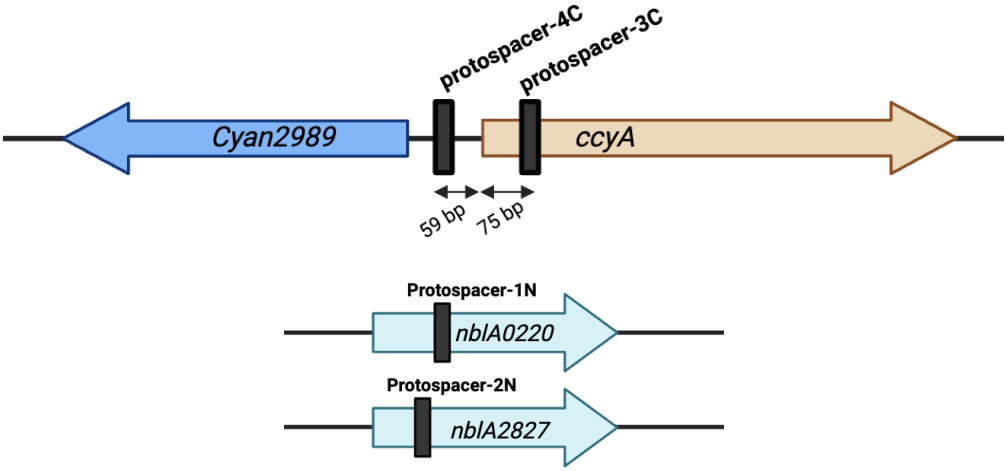

Figure 11: Schematic representation of protospacers on the chromosome to which the dCas12a is guided to bind and inhibit transcription. The small black arrows represent the distance between the protospacer and the start of the ccyA gene. Top: Repression of ccyA on C.7425 chromosome. Bottom: Repression of nblA0220 and nblA2878 on C.7425 chromosome.

To guide the Cas effector protein, in both deletion and repression, spacers for the CRISPR array was chosen based on a number of criteria taken from the CRISPR/Cas12a study by Niu *et al.* (2019). The PAM site had to be 5′-KTTV-3′ (K = T or G, while V = C, G, or A), the protospacer sequence directly downstream of PAM had to be 22 bp long and should not contain more than eight repeated GC pairs.

2 Materials and Methods

2.1 Bacterial Strains and Culture Conditions

Cyanothece sp. PCC 7425 (C.7425) and *Synechococcus elongatus* PCC 7942 was cultured in mineral media (MM), see Appendix A for composition, in 30ºC under continuous agitation of 140 rpm (Infors rotary shaker) at 2000-2500 lux, 31.25 µE. $m^{-2}.s^{-1}$. *Cyanothece* sp. PCC 7425 was also cultured in the same T°, light and agitation conditions in BG11 media, see Appendix A for composition. *E. coli* strains NEB10-beta (New England Biolabs), used for cloning, and CM404, used as helper strain for triparental conjugation, were cultured in both liquid and solid LB medium at 30ºC (CM404) and 37ºC (NEB10-beta). For overnight cultures, *E. coli* strains in liquid LB were put in incubator with 180 rpm continuous agitation. For selection of *E. coli* strains, the following antibiotic concentrations were used; kanamycin (Km) 50 µg/mL, streptomycin (Sm) 25 µg/mL, spectinomycin (Sp) 75 µg/mL. For selection of *Cyanothece* sp. PCC 7425 strains; Km 25-50 µg/mL, Sm 5-10 µg/mL, Sp 5-10 µg/mL. For selection of *Synechococcus elongatus* PCC 7942 strains Sm 5 µg/mL and Sp 5 µg/mL. See Appendix B, for a list specifying strains and plasmids used.

2.2 Conjugative Transfer of Plasmids into *Cyanothece* sp. PCC 7425

For introduction of plasmids to C.7425 a triparental conjugation is utilized based on the method by Chenebault *et al.* (2020) see figure 6. Three mL cultures of NEB10-beta, harbouring the plasmid for transfer, and CM404, harbouring the RP4 plasmid, were grown overnight. The next day, they were washed twice with LB, and concentrated in fresh LB to a concentration of $1.3*10^9$ cells/mL based on OD_{600} measurement after wash. C.7425 culture was grown to exponential growth phase, OD_{750} ~ 0.6-9, and based on initial OD_{750} measurement the culture was washed and concentrated $1.25*10^7$ cells/mL. Then the cultures were mixed to a ratio of 3:1:1, 100 µL C.7425, 30 µL NEB10-beta, and 30 µL CM404. For negative control, 100 µL C.7425 and 60 µL CM404 was mixed. From the mixes, aliquots of 30 µL were spotted on non-selective MM-agar plates and incubated at 30°C for 48-72 hours in 2500 lux light.

After incubation, spots where then taken individually and resuspended in 100 µL MM and streaked on selective MM-plates. The plates were then incubated under standard conditions for 2-3 weeks. When colonies had appeared, they were resuspended in 10 µL fresh MM and spotted onto selective MM-plates. After appearance of clones, they were picked and verified by PCR (polymerase chain reaction) and DNA sequencing by Mix2Seq kit (Eurofins Genomics). For primers used, see Appendix C, and for PCR reaction mix and settings, see Appendix D and E.

2.3 Phenotypic Characterization of Strains Overexpressing *ccyA*

For the growth experiment with C.7425 strains overexpressing *ccyA* from pC derived plasmids, see Appendix B for plasmids, cultures were first grown in BG11 in standard conditions to OD_{750} ~3-3.8. They were then washed twice with BG11 without calcium (BG11-Ca), see Appendix A. The experiment was set up in 250 mL Erlenmeyer flasks with 50 mL of culture or 50 mL of BG11-Ca, as abiotic control. Based on OD_{750} measurement after the washes, the cultures were diluted to OD_{750} ~0.1 in fresh BG11-Ca supplemented with $CaCl_2$ solutions, 20- or 100 mM, to a total concentration of either 50- or 250 µM Ca^{2+}. The abiotic controls were also supplemented with the same $CaCl_2$ solutions.

The flasks were then incubated under standard conditions for three weeks. Every two days, expect over weekends, sampling of the flasks was done, see Appendix F "Sampling protocol for growth experiment with *ccyA* overexpression mutants" for protocol. Before taking a sample, sterile nuclease-free water was added to each flask based on how much liquid was lost in evaporation since last sampling. Then, from each flask for the first two weeks, three mL samples were taken, whereupon one mL was used for pH and OD_{750} measurements and the other two mL for inductively coupled plasma mass spectrometry (ICP-MS). To prepare samples for ICP-MS analysis, they were first filtered using Millex® PVDF syringe filter (0.22 µm pore size) into 15 mL Falcon® tubes and supplied with one drop 70% HNO_3 (Sigma Aldrich), whereupon they were stored at 4°C. The pH and OD_{750} measurements were done right after sampling. For the last week of sampling, only one mL samples were taken for pH and OD_{750} measurements. The pH measurements were conducted on 900 µL samples in room temperature using Mettler Toledo SevenCompact™ pH meter S210 with a Metrohm Biotrode (6.0224.100) electrode. The samples for ICP-MS analysis were sent to Institut de Minéralogie, Physique des Matériaux et Cosmochimie (IMPMC) who conducted the measurements.

2.4 Construction and Selection of CRISPR/Cas12a and CRISPRi-dCas12a Plasmids

The pSL2680 derived plasmids for CRISPR/Cas12a mediated deletion of *ccyA* in C.7425 were, previous to the project (unpublished data, LBBC), constructed in the LBBC lab and therefore ready for triparental conjugation into C.7425. The methods explained here concerns therefore the pSL2680 derived plasmids for deletion of *CAX* genes in C.7425 and the pSL3287 derived plasmids for repression of genes in C.7425.

Both base plasmids were gifted from Himadri Pakrasi, pSL2680 (Addgene plasmid # 85581 ; http://n2t.net/addgene:85581 ; RRID:Addgene_85581) and pSL3287 (Addgene plasmid # 139750 ; http://n2t.net/addgene:139750 ; RRID:Addgene_139750).

The plasmids were first isolated from NEB10-beta cultures using NucleoSpin® Plasmid EasyPure kit, then linearized by restriction digestion with *Aar*I (Thermo-Fischer) according to set up in table 2. The tubes were incubated for four hours at 37 °C then heat inactivated at 65 °C for 20 minutes. The digestion was confirmed by agarose gel electrophoresis (1% agarose).

Table 2: AarI restriction digestion setup for 50 µL reaction.

Component	**Volume of component for 50 µL reaction**
Nuclease-free H_2O	Add to 50 µL
10X Buffer *Aar*I	5 µL
50X Oligonucleotides	1 µL
*Aar*I	2 µL
DNA	Add volume to a total of 2 µg DNA

The spacer sequences to be inserted in the CRISPR arrays of pSL2680 and pSL3287 were first annealed from phosphorylated oligos ordered from IDT, see Appendix C. In a PCR tube, 2 µL respectively of the oligo pairs were added to 16 µL nuclease-free water. The mix was incubated at 95 °C for five minutes and then cooled to 4 °C with a rate of 0,1 °C per second, whereupon it was stored in 4°C. The linearized base plasmids were then ligated with the annealed CRISPR arrays by T4 DNA ligase (New England Biolabs) according to protocol M0202. For the incubation part of the M0202 protocol, the reaction mixes were left overnight on the lab-bench (room temperature). The annealed plasmids containing the CRISPR arrays

were then transformed following the High Efficiency Transformation Protocol using NEB® 10-beta Competent E. coli (High Efficiency). The transformation mix was plated on LB plates containing Km 50 µg/mL, IPTG 0.1 M and X-gal (5-Bromo-4-chloro-1H-indol-3-yl β-D-galactopyranoside) 20 mg/mL. When white colonies had appeared, they were verified with colony PCR and sequencing, see Appendix E and F for PCR set-up and Appendix C for primers. The clones housing pSL3287 derivative plasmids for CRISPRi with their correct CRISPR array inserts were then conjugated into their respective C.7425 culture using the triparental conjugation method described above.

To make the editing plasmids for deletion and HDR, the homology repair template had to be inserted into the pSL2680 derivatives housing their respective CRISPR arrays. First, plasmids were isolated using NucleoSpin® Plasmid EasyPure kit from their NEB10-beta cultures. They were then linearized by restriction digestion with *Sal*I (New England Biolabs), see table 3 for set-up. The tubes were incubated for one hour at 37 °C then heat inactivated at 65 °C for 20 minutes. To confirm digestion, samples were run on agarose gel electrophoresis (1% agarose).

Table 3: SalI restriction digestion setup for 50 µL reaction.

Component	**Volume of component for 50 µL reaction**
Nuclease-free H_2O	Add to 50 µL
10X NEBuffer r3.1	5 µL
*Sal*I	1 µL
DNA	Add volume to a total of 1 µg DNA

The homology repair template for each HDR was made up of an Sm^R/Sp^R cassette for selection flanked by two homologous platforms. First, the Sm^R/Sp^R cassette was amplified by PCR from a pC-plasmid using partially overlapping primers to the homologous platforms, see Appendix C. The PCR product was verified by agarose gel electrophoresis (1% agarose) and purified by NucleoSpin® Plasmid EasyPure kit before assessing the quality and quantity of DNA using NanoDrop (ThermoFisher Scientific). The homology platforms were also amplified by PCR from C.7425 chromosome using partially overlapping primers to the selection cassette and the plasmid, see Appendix C. These PCR products underwent the same verification as for the selection cassette. All the primers for the homology repair template were designed by NEBuilder. To insert the homology repair template, Gibson Assembly was performed using the NEB HiFi DNA Assembly Cloning Kit (New England BioLabs). The

reaction was set-up according to the Gibson Assembly® Protocol (E5510), see table 4. The tubes were incubated at 50 °C for one hour then transformed into competent NEB10-beta cells. Selection was performed by spotting on LB plates containing Km 50 µg/mL, Sm 25 µg/mL, and Sp 75 µg/mL. The clones were then verified by PCR, see Appendix C for primers, and sequencing. Following verification, the finished editing plasmids were conjugated into their respective C.7425 cultures using the triparental conjugation method.

Table 4: Gibson assembly reaction set-up according to protocol E5510 (New Englands Biolabs) using 4 fragments for assembly. The molar ratio for the fragments are 1:1 insert:vector.

Component	Volume of component for 20 µL reaction
Total Amount of Fragments	X µL (0.2-1 pmols)
Gibson Assembly Master Mix (2X)	10 µL
Deionized H_2O	Add to 20 µL

2.5 Experimental Design for Repression of *nblA* in *Cyanothece* sp. PCC 7425 Using CRISPRi-dCas12a

For repression of *nblA* in C.7425 using CRISPRi-dCas12a plasmids, see Appendix B, the strains prior to experiment were grown in BG11 under standard conditions. To start the experiment the strains were inoculated to OD_{750}~0.2 in 10 and 12 mL BG11 using 50 mL Erlenmeyer flasks and incubated under standard conditions for 48 hours. The cultures containing the CRISPRi plasmids were subjected to 4 mM IPTG at inoculation. After 48 hours, cultures were washed twice, with BG11-NO_3 for the 12 mL cultures and BG11 for the 10 mL cultures. From the 12 mL cultures, 2 mL was taken and spotted on solid BG11 and BG11-NO_3 plates, with or without IPTG, in spots of 50 µL, 40 µL, and 30 µL. The plates were then incubated at 30ºC in 2500 lux for 72 hours and pictures was taken after 72 hours. The remaining 10 mL of the cultures was pipetted into four wells respectively on a Falcon® 12-well cell culture plate to a volume of 2.5 mL per well. Three of the wells for each culture was then inducted with 2 mM, 5 mM, and 10 mM IPTG respectively before incubation in standard conditions for 72 hours. For the 10 mL cultures washed with BG11, they were inducted with the same IPTG concentrations but incubated at 30ºC in ~7000 lux and 140 rpm continuous agitation (Infors rotary shaker). Pictures of the multi-well plates were taken right after induction, after 24 hours and after 72 hours. For making of absorption spectras, 100 µL samples were taken throughout the experiment and the measurements were made directly after sampling using a Shimadzu UV-1800 spectrophotometer.

3 Results

3.1 *Cyanothece* sp. PCC 7425 Strains Overexpressing *ccyA*

To study if overexpression of *ccyA* in an iACC-forming strain would have any effect, C.7425 overexpression mutants were grown for three weeks in standard photoautotrophic conditions in BG11 containing either 50 µM or 250 µM Ca^{2+}. pH and OD_{750} were measured every other day, expect weekends. ICP-MS was done on samples from the first two weeks to measure changes of Ca^{2+} amount in media.

3.1.1 Limited Growth on Media with 50 µM Ca^{2+}

As previously established by De Wever *et al*. (2019), C.7425 have a limited growth on media containing 50 µM Ca^{2+}. This holds true in this experiment as well, see figure 12 for OD_{750} measurements. The lower Ca^{2+} concentration causes the cultures to reach an OD_{750} between 1 and 2 while the standard concentration, 250 µM Ca^{2+}, has a higher OD_{750} between 3 and 4,2 after three weeks of growth. No notable differences between the control strains, and the overexpression mutants can be seen as they follow much the same pattern of growth, independent of Ca^{2+} concentration in media. The average difference comparing wildtype to the mutants grown in limited calcium concentration showed a greater difference between wildtype and C.7425 harboring the empty pC plasmid, 0.6 units of OD_{750}, than between the wildtype and the mutants overexpressing *ccyA*, 0.28 to 0.53 units of OD_{750}. For cultures grown in standard concentration the average differences between mutants overexpressing *ccyA* and wildtype is much greater at 0.16 to 0.57 units of OD_{750}. However, in figure 12 the growth measurements follow much the same pattern. Therefore, no to minimal effect on growth based on overexpression of *ccyA* can be seen in limited or standard Ca^{2+} concentration for this one replicate. Pictures of the culture flasks taken throughout the three weeks show that the mutants grown in lower Ca^{2+} had a light-yellow colour and were lighter than the wildtype at day 22, see figure 13.

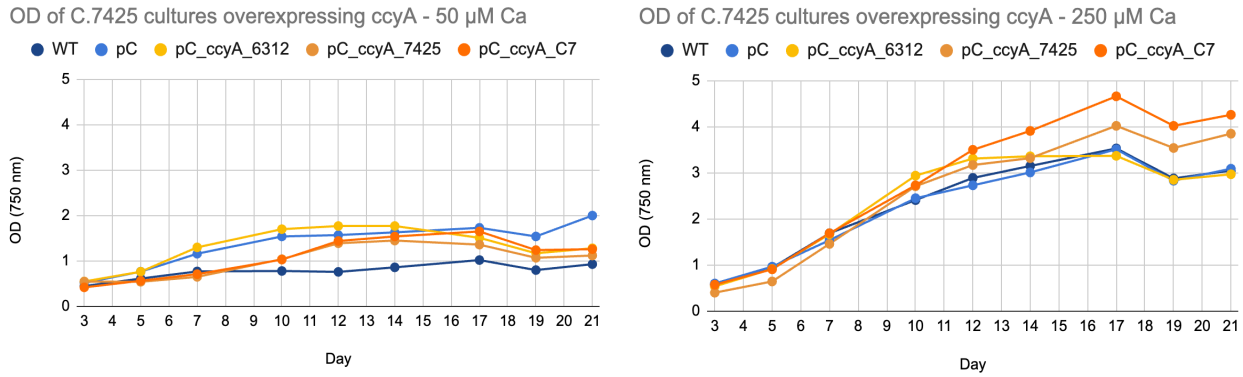

Figure 12: Growth of C.7425 strains measured by OD_{750} over three weeks in standard conditions in BG11 media containing either 50 µM Ca^{2+} (top graph) or 250 µM Ca^{2+} (bottom graph). The two controls are wildtype, "WT", and C.7425 harbouring the base pC plasmid without modifications, "pC". The mutant strains overexpressing the ccyA gene: from Synechococcus sp. PCC 6312 is "pC_ccyA_6312", from Cyanothece sp. PCC 7425 is "pC_ccyA_7425", and Gloeomargarita lithophora C7 is "pC_ccyA_C7.

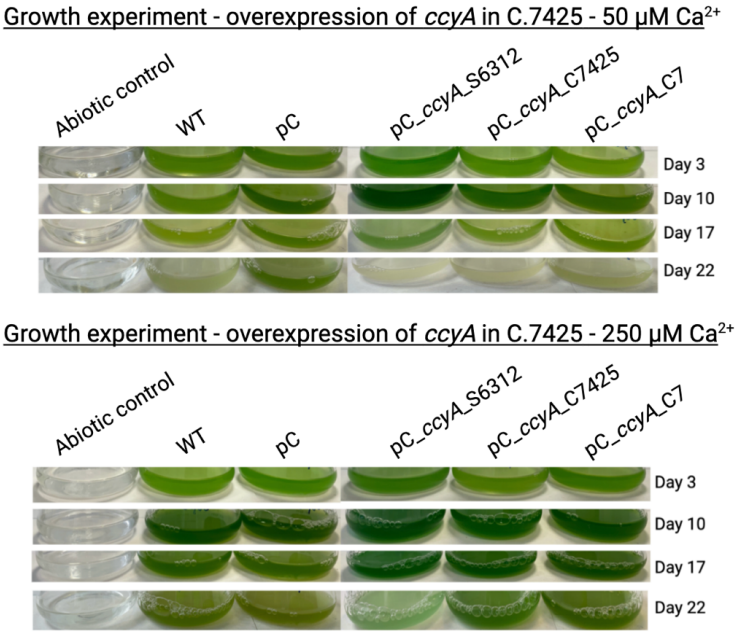

Figure 13: Pictures taken of cultures throughout the experiment, from day 3 to day 22. "Abiotic control" contain no cells, while "WT" represents wildtype control and "pC" cells propagating the empty pC vector. The mutant strains overexpressing the ccyA gene: from Synechococcus sp. PCC 6312 is "pC_ccyA_6312", from Cyanothece sp. PCC 7425 is "pC_ccyA_7425", and Gloeomargarita lithophora C7 is "pC_ccyA_C7.

3.1.2 Overexpression Mutants in Media with 250 µM Ca^{2+} Show Differences in Ca^{2+} Uptake and pH of Media

For the strains grown in 250 µM Ca^{2+} notable changes in pH and Ca^{2+} uptake from media can be seen for the overexpression mutants around seven to ten days of growth, see figure 14. For mutants overexpressing *ccyA* from *Synechococcus* sp. PCC 6312 ($pC_{ccyAS6312}$) and C.7425 ($pC_{ccyAC7425}$) their pH rose 2.22 and 2.59 units respectively, from day three to their peak at day seven. The overexpression mutant with *ccyA* from *Gloeomargarita lithophora* C7 (pC_{ccyAC7}) had a peak at day ten with a pH increase of 1.61 units. The average difference between the mutants and the wildtype shows that the C.7425 harbouring the empty pC vector (pC) has a smaller difference in pH compared to wildtype than those overexpressing *ccyA*, see table 5. The peaks in pH correlates well with the peaks of Ca^{2+} uptake for the mutants, see figure 14. Both measurements peak at around day seven to ten and then drop off towards day 14. The control strains, wildtype and pC, can be seen containing a low amount of Ca^{2+} in the media, i.e. the percentage of Ca^{2+} available in the media that has been taken up stays high over time. While Ca^{2+} in the media of the mutants increases after day seven and reaches a value near the value of the first sampling at day three. Table 5 shows the average difference in Ca^{2+} uptake between mutants and wildtype. The Ca^{2+} uptake measurements, similar to the pH measurements, showed a greater difference between the wildtype and mutants overexpressing *ccyA* than between the wildtype and pC.

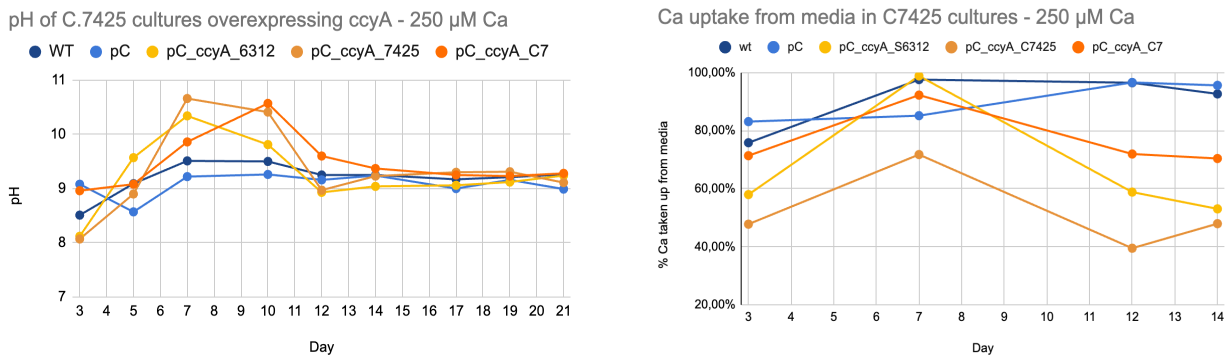

Figure 14: Top: pH of media from samples taken throughout three weeks of growth in standard conditions in BG11 media containing 250 µM Ca^{2+}. Bottom: Percentage of Ca^{2+} taken up from media at the time point of sampling based on the amount of Ca^{2+} in the abiotic control. Samples for measuring Ca in each flask with ICP-MS were taken throughout the first two weeks. In both graphs, the two control strains are wildtype, "WT", and C.7425 harbouring the base pC plasmid without modifications, "pC". The mutant strains overexpressing the ccyA gene from Synechococcus sp. PCC 6312 is "pC_ccyA_6312", from Cyanothece sp. PCC 7425 is "pC_ccyA_7425", and Gloeomargarita lithophora C7 is "pC_ccyA_C7.

Table 5: Average difference between wildtype and mutants in pH and percentage of Ca^{2+} uptake for cultures grown in standard conditions in BG11 media containing 250 µM Ca^{2+}. Calculated based on the difference between mutant and wildtype at each sample measurement and then averaged.

Mutant compared to wildtype	Average difference in pH measurements between wildtype and mutant, units in pH	Average difference in Ca^{2+} uptake measurements between wildtype and mutant, units in percentage
pC	0.25	0.06
$pC_{ccyAS6312}$	0.3	0.24
$pC_{ccyAC7425}$	0.37	0.39
pC_{ccyAC7}	0.27	0.14

The strains grown in limiting Ca^{2+} concentration showed no notable differences in pH and Ca^{2+} uptake between the control strains and the overexpression mutants, see figure 15. No clear peak at day seven could be seen as previously shown in standard Ca^{2+} concentration. Although, regarding Ca^{2+} uptake for overexpression mutant with $pC_{ccyA6312}$, the concentration in the media increased significantly after day 12. Comparing the average differences between the mutants and the wildtype, see table 6, shows smaller differences in calcium uptake measurements than for those grown in standard calcium concentration, see table 5. However, table 6 also indicates that the differences in pH compared to wildtype is generally greater for these cultures but the values are closer to each other suggesting a similar difference to wildtype.

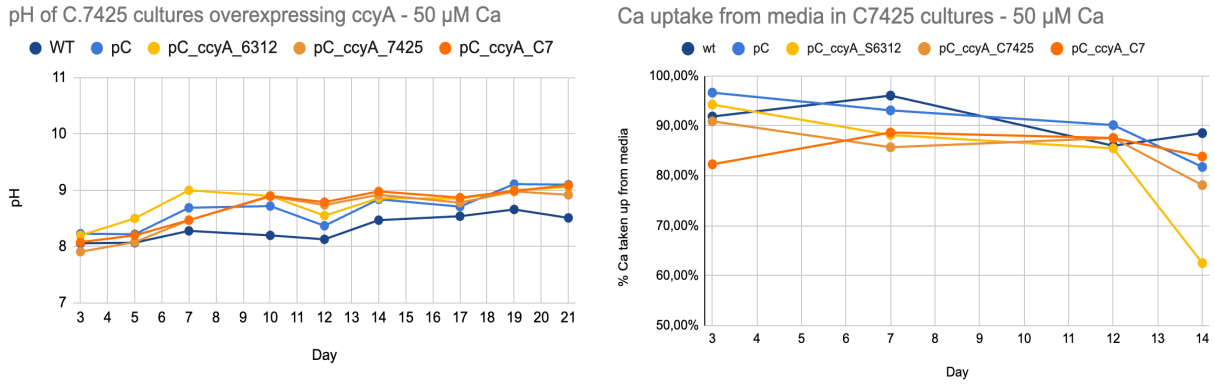

Figure 15: Top: pH of media from samples taken throughout three weeks of growth in standard conditions in BG11 media containing 50 µM Ca^{2+}. Bottom: Percentage of Ca^{2+} taken up from media at the time point of sampling based on the amount of Ca^{2+} in the abiotic control compared to the strains. Samples for measuring Ca^{2+} in each flask with ICP-MS were taken throughout the first two weeks. In both graphs, the two control strains are wildtype, "WT", and C.7425 harbouring the base pC plasmid without modifications, "pC". The mutant strains overexpressing the ccyA gene from Synechococcus sp. PCC 6312 is "pC_ccyA_6312", from Cyanothece sp. PCC 7425 is "pC_ccyA_7425", and Gloeomargarita lithophora C7 is "pC_ccyA_C7.

Table 6: Average difference between wildtype and mutants in pH and percentage of Ca^{2+} uptake for cultures grown in standard conditions in BG11 media containing 50 μM Ca^{2+}. Calculated based on the difference between mutant and wildtype at each sample measurement and then averaged.

Mutant compared to wildtype	Average difference in pH measurements between wildtype and mutant, units in pH	Average difference in Ca^{2+} uptake measurements between wildtype and mutant, units in percentage
pC	0.34	0.047
$pC_{ccyAS6312}$	0.44	0.092
$pC_{ccyAC7425}$	0.34	0.058
pC_{ccyAC7}	0.38	0.058

3.2 CRISPR/Cas12a Mediated Deletion of *ccyA* and *CAX* in *Cyanothece* sp. PCC 7425

For verifying deletion of *ccyA* in C.7425 using the CRISPR/Cas12a plasmids, clones were first taken from spots on the selection plate after triparental conjugation with the p$\Delta ccyA_{C7425}$crRNA1 and p$\Delta ccyA_{C7425}$crRNA2 and incubated in MM with 5 μg/mL Sm/Sp in standard conditions. After cultures had turned green samples were taken for verification with PCR, see figure 16. Using one primer on the chromosome, outside of the homology repair template and one primer on the selection cassette yielded a PCR product of correct size, 1.5 kb, from both clones but not from wildtype negative control. This shows that deletion of *ccyA* from at least one chromosome copy was successful. However, using primers that are both on the chromosome, outside of the homology repair template, resulted in bands corresponding to the size of the wildtype copy, 2.28 kb, for all samples. This shows that both mutants still harbours wildtype chromosome copies possessing an intact *ccyA* gene. However, looking at the higher intensity of the bands on gel for clone 1, p$\Delta ccyA_{C7425}$crRNA1 it might have better chromosome segregation than clone 2, p$\Delta ccyA_{C7425}$crRNA2.

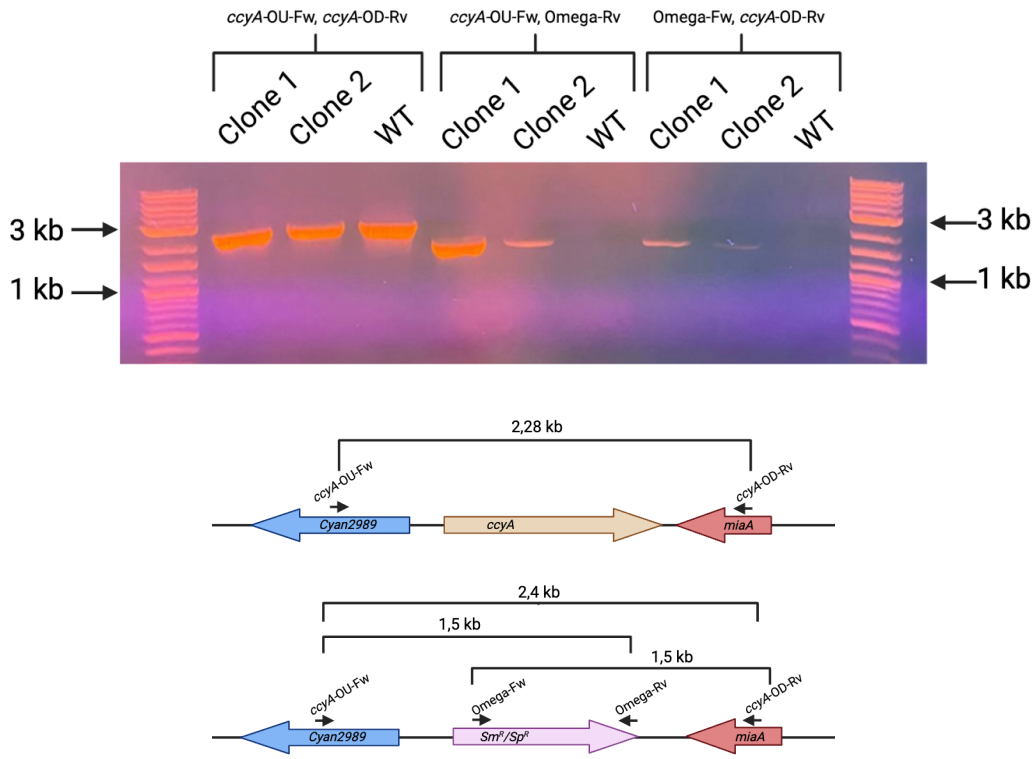

Figure 16: Top: UV-image of PCR products on 1% agarose gel. Samples used for PCR were taken from cultures of MM with 5 µg/mL Sm/Sp. Clone 1: C.7425 housing pΔccyA$_{C7425}$crRNA1. Clone 2: C.7425 housing pΔccyA$_{C7425}$crRNA2. WT indicates control, wildtype. Primers used are written on top and the corresponding PCR product bands are sorted by brackets. Bottom: Schematic representations of C.7425 chromosome in which the top scheme represents a wildtype copy and the bottom scheme represents a deleted copy with HDR using the template containing an Sm^R/Sp^R cassette. Genes are represented by coloured arrows pointing at the direction of transcription. Primers are represented by the black arrows and black brackets represents the amplified PCR product using mentioned primers.

For verifying deletion of *CAX3000* and *CAX3001* in C.7425, samples for PCR were taken from spots on the selection plate after triparental conjugation with the pΔ*CAX*$_{C7425}$crRNA1 and the pΔ*CAX*$_{C7425}$crRNA2 plasmids. The PCR product was amplified using primers that bind on the chromosome outside of the homology repair template. Figure 17 show that the bands on the gel of all the clones correspond to the size of a successful deletion and HDR, 2.6 kb. This means that both spacers chosen for guiding the Cas12a and the pSL2680 CRISPR/Cas12a system was successful in deleting the two *CAX* genes in C.7425.

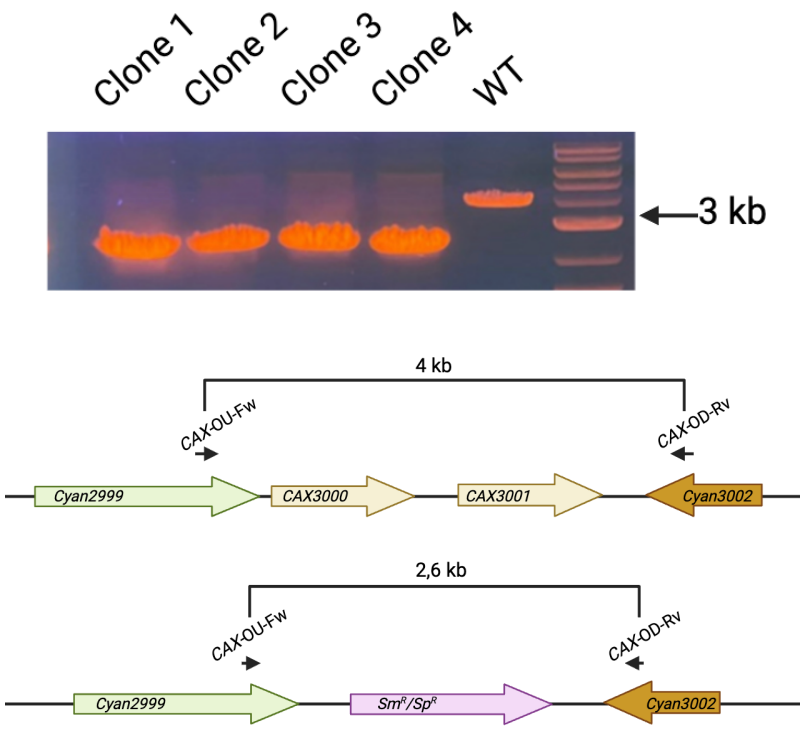

Figure 17: Top: UV-image of PCR products on 1% agarose gel. Samples used for PCR were taken from spots on the selection plate after triparental conjugation. Clone 1 and 2: C.7425 housing pΔCAX$_{C7425}$crRNA1. Clone 3 and 4: C.7425 housing pΔCAX$_{C7425}$crRNA2. WT indicates positive control, wildtype. Primers used were CAX-OU-Fw and CAX-OD-Rv (see Appendix C). Bottom: Schematic representations of C.7425 chromosome in which the top scheme represents a wildtype copy and the bottom scheme represents a deleted copy with HDR using the template containing an Sm^R/Sp^R cassette. Genes are represented by coloured arrows pointing at the direction of transcription. Primers are represented by the black arrows and black brackets represent the amplified PCR product using mentioned primers.

3.3 CRISPRi IPTG-Inducible Repression of Control Gene Showed No Visible Phenotype in *Cyanothece* sp. PCC 7425

To determine if the IPTG inducible CRISPRi system would function in C.7425, a control experiment using *nblA* was conducted first. This step was taken before starting the analysis of *ccyA* repression. The control experiment was chosen because its results are visibly noticeable, unlike *ccyA* repression, which requires more time-consuming RT-PCR (reverse transcription-polymerase chain reaction) for confirmation. Due to the negative results described below for the control experiment, analysis of *ccyA* repression was never initiated.

Repression of *nblA* in model cyanobacteria during nitrogen starvation has previously shown to produce a null phenotype that stays blue-green instead of turning yellow, like the wildtype due to degradation of its phycobilisomes (Baldanta *et al.* 2022; Sun Young Choi & Han Min Woo 2020). Cultures were first grown in BG11 with 4 mM IPTG for two days before being subjected to BG11-NO_3 and induced with varying IPTG concentrations and incubated in standard conditions for three days. Figure 18 shows pictures taken throughout the three days of incubation in nitrogen deficient media. No blue-green phenotype was visible with no apparent difference between the wildtype and the mutants depending on the IPTG concentration.

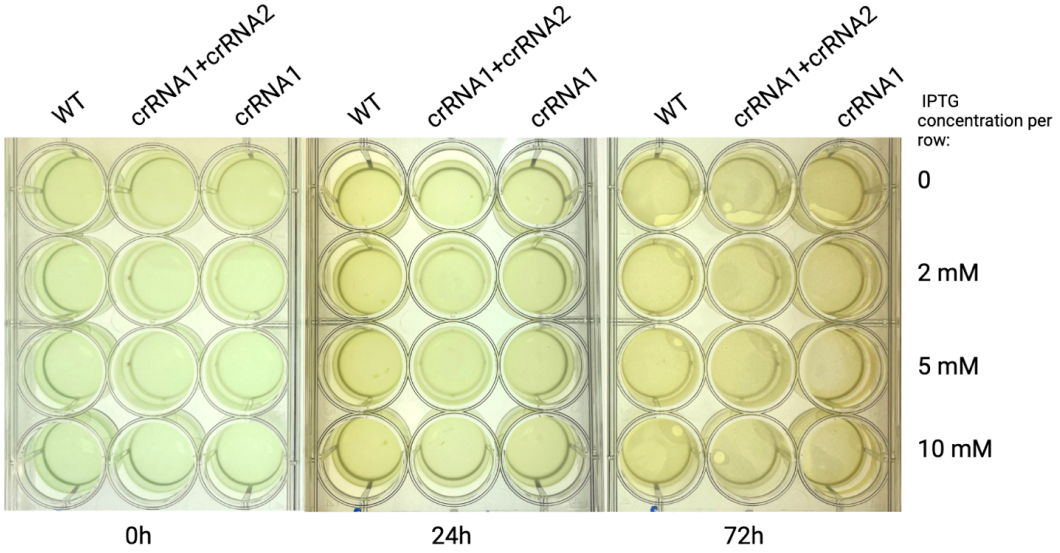

Figure 18: Pictures showing one multi-well plate incubated at standard conditions with BG11-NO_3 (nitrogen starvation) over the course of 72 hours. Each column contains a C.7425 culture: a positive control being wildtype "WT", "crRNA1+crRNA2" housing the pSL3287$_{nblAC7425}$crRNA1-crRNA2 plasmid, "crRNA1" housing the pSL3287$_{nblA0220C7425}$crRNA1 plasmid. Each row was inducted at 0 hours with different IPTG concentrations mentioned on the right side of the pictures.

Since no blue-green phenotype could be seen with the naked eye, absorption spectra were made of samples taken before or after nitrogen starvation with or without induction with IPTG. The phycobilisomes contain phycocyanin with an absorption maximum at 620 nm that can be used as a marker for phycobilisome content (Kasinak *et al.* 2014). Figure 19 shows absorption spectra of samples throughout the experiment where upon comparing the OD at 620 nm shows no difference between the wildtype and the two mutants in nitrogen starvation with and without 10 mM IPTG. Looking at the same figure, samples taken before nitrogen starvation (blue and light blue lines), 24 hours after nitrogen starvation (yellow and orange lines) with and without IPTG showed similar peaks at 620 nm indicating no degradation of the phycobilisomes. Comparing the wildtype (green lines) and the mutant (orange lines) after 24 hours of nitrogen starvation and 10 mM IPTG show no difference in OD at 620 nm either, see figure 19. The gap between measurements taken before nitrogen starvation (blue and light blue lines) and the ones taken after 24 hours starvation could be due to the overall degradation of the light harvesting complexes during nitrogen starvation, especially at 620 nm, which indicates NblA degrading the phycobilisomes. Therefore, these results suggest that the CRISPRi system has no effect on *nblA* repression in C.7425 during nitrogen starvation.

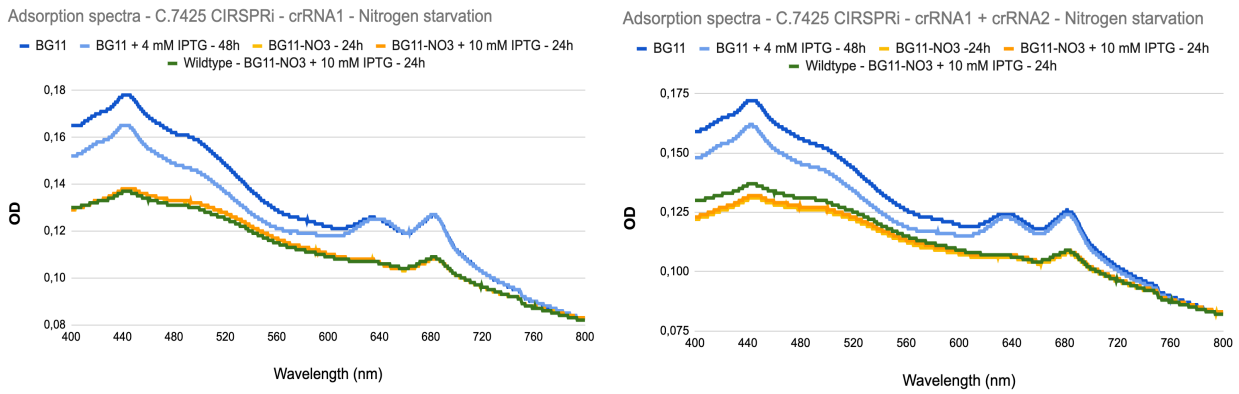

Figure 19: Absorption spectra of samples taken throughout the CRISPRi experiment for repression of nblA in C.7425 with nitrogen starvation. The name of the samples is described as follows: BG11: Right after inoculation in BG11 media and before induction with IPTG. BG11 + 4 mM IPTG -48h: After 48 hours incubation in BG11 media with 4 mM IPTG in Erlenmeyer flask. BG11-NO3 -24h: 24 hours after inoculation in BG11-NO_3 media in multi-well plate. BG11-NO3 + 10 mM IPTG -24h: 24 hours after inoculation in BG11-NO_3 media with 10 mM IPTG in multi-well plate. Wildtype – BG11-NO3 + 10 mM IPTG -24h: The positive control, wildtype strain, 24 hours after inoculation in BG11-NO_3 media with 10 mM IPTG in multi-well plate. Left: Regards the mutant housing the pSL3287$_{nblA0220C7425}$crRNA1 plasmid. Right: Regards the mutant housing the pSL3287$_{nblAC7425}$crRNA1-crRNA2 plasmid.

The phycobilisomes are also known to be degraded during conditions of high light to prevent damage from excess excitation of the photosystems (Sendersky *et al.* 2015). Since the physiology of C.7425 is poorly studied, this stress condition was applied to see it would give a phenotype with repression of *nblA* instead of nitrogen starvation condition. Therefore, an experiment was conducted where the strains were subjected to highlight stress, ~7000 lux, in normal BG11 but with the same incubation time and IPTG concentrations. Figure 20 shows pictures taken throughout the experiment where no visible phenotype could be seen again, similar to nitrogen starvation conditions. Absorption spectra of samples were also made in the same procedure as for nitrogen starvation experiment, see figure 21. In these spectra no difference in OD between the induced mutants and the wildtype could be seen at 620 nm after 24 hours in highlight with 10 mM IPTG, see orange and green lines in figure 21. Similar to the nitrogen starvation experiment, a gap between samples taken before and after 24 hours of highlight stress can be seen possibly due to the degradation of the light harvesting complexes.

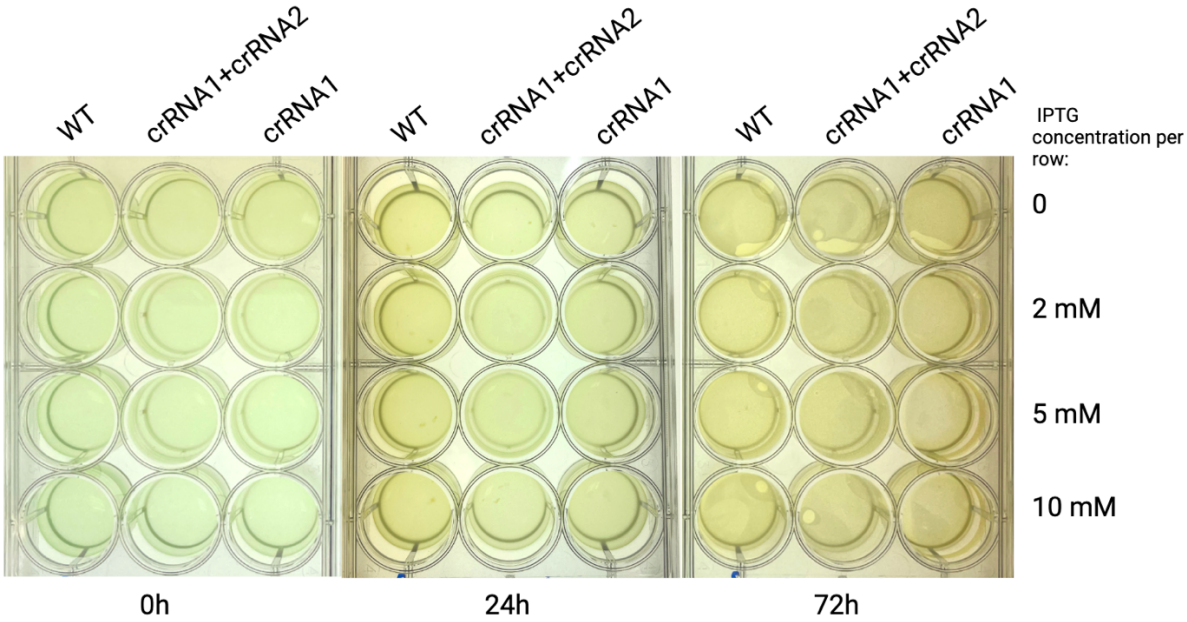

Figure 20: Pictures showing one multi-well plate incubated at ~7000 lux (highlight stress) with BG11 over the course of 72 hours. Each column contains a C.7425 culture: a positive control being wildtype "WT", "crRNA1+crRNA2" housing the pSL3287$_{nblAC7425}$crRNA1-crRNA2 plasmid, "crRNA1" housing the pSL3287$_{nblA0220C7425}$crRNA1 plasmid. Each row was inducted at 0 hours with different IPTG concentrations mentioned on the right side of the pictures.

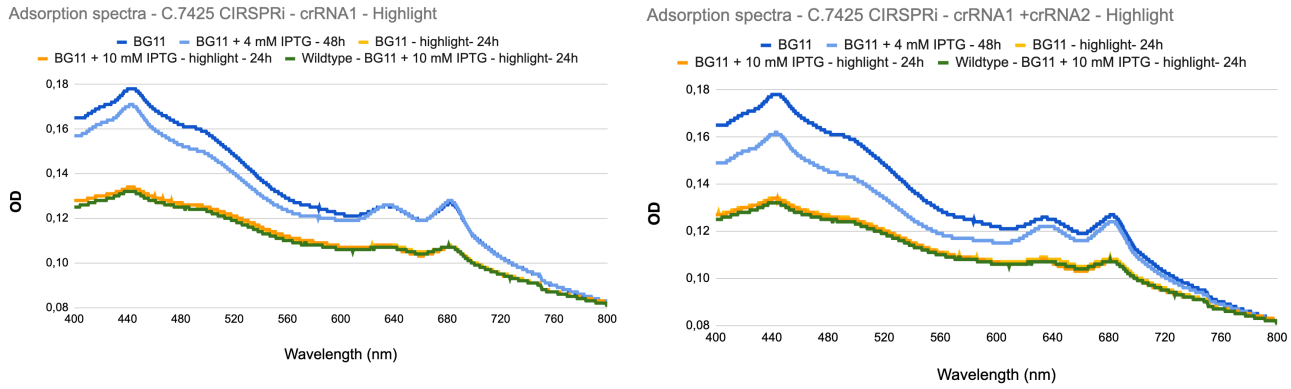

Figure 21: Figure X: Absorption spectra of samples taken throughout the CRISPRi experiment for repression of nblA in C.7425 with highlight stress. The name of the samples is described as follows: BG11: Right after inoculation in BG11 media and before induction with IPTG. BG11 + 4 mM IPTG -48h: After 48 hours incubation in BG11 media with 4 mM IPTG in Erlenmeyer flask. BG11-highlight -24h: 24 hours after inoculation in BG11 media in highlight in multi-well plate. BG11 + 10 mM IPTG - highlight - 24h: 24 hours after inoculation in BG11 media with 10 mM IPTG in highlight in multi-well plate. Wildtype – BG11 + 10 mM IPTG - highlight - 24h: The positive control, wildtype strain, 24 hours after inoculation in BG11 media with 10 mM IPTG in highlight in multi-well plate. Left: Regards the mutant housing the pSL3287$_{nblA0220C7425}$crRNA1 plasmid. Right: Regards the mutant housing the pSL3287$_{nblAC7425}$crRNA1-crRNA2 plasmid.

4 Discussion

This section discusses the results presented in the results section as well as how to move forward with the experiments based on their outcome. This section is therefore divided based on the three main genetic strategies employed for analysing the function of *ccyA* in C.7425, overexpression, deletion, and repression.

4.1 Hypotheses on the Role of *ccyA* in *Cyanothece* sp. PCC 7425 Based on Overexpression Experiment

The relationship between pH and Ca^{2+} uptake appears to be influenced by overexpression of *ccyA* in C.7425 in standard Ca^{2+} concentration of BG11 (250 μM), see figure 14. An increase of extracellular pH is thought to be connected to extracellular biomineralization (Görgen *et al.* 2020), where carbonic anhydrases (CA) convert bicarbonate (HCO_3^-) to CO_2 and OH^-, exporting OH^- and importing H^+ to balance intracellular pH. The observed pH peak of the mutants may be attributed to CcyA acting as a bicarbonate importer. This could lead to increased bicarbonate uptake and subsequent production of OH^-, resulting in the pH increase. Although, another unresolved aspect of the experiment is why the overexpression of *ccyA* leads to a release of Ca^{2+} into the media after the pH peak, rather than the retention as seen in the controls, wildtype and C.7425 harbouring the empty pC plasmid. Further investigations are required to understand the cause of this behaviour. The current findings are based on a single replicate, highlighting the need for more replicates to confirm the results. Future experiments should also include SEM imaging before, during, and after the observed pH and Ca^{2+} uptake peaks (between day seven and ten of growth). This imaging will help in checking possible changes in granules number and size as well as provide insights into determining whether there is an increase in extracellular or intracellular biomineralization. Despite observed biochemical changes, the overexpression of *ccyA* did not significantly impact the growth of C.7425 under either standard or limiting Ca^{2+} conditions. This suggests that while overexpression of *ccyA* might influence biomineralization processes, its overexpression does not hinder cellular proliferation.

4.2 CRISPR/Cas12a Can Be Used for Gene Manipulation in *Cyanothece* sp. PCC 7425, and *ccyA* is Possibly Crucial to the Growth of *Cyanothece* sp. PCC 7425

The use of the CRISPR/Cas12a system in this project in C.7425 has shown significant promise for genomic modifications, manifested by the successful deletion of three genes with HDR, one for glutathione reductase (unpublished data, LBBC) and two *CAX* genes (this project). Concerning *ccyA*, the results indicate that the CRISPR/Cas12a with HDR system successfully deleted the *ccyA* gene of at least one copy on the chromosome in C.7425. However complete chromosome segregation was not achieved, as wildtype (WT) copies of *ccyA* was still detectable with PCR. The persistence of WT copies of the chromosome, even in the presence of high antibiotic concentrations suggests that *ccyA* is crucial to C.7425 life. However, the mutants with partially segregated chromosomes might still provide valuable insights into intracellular biomineralization and the role of *ccyA*. Many unsegregated (heteroploidy) mutants of cyanobacteria turned out to have a phenotype allowing researcher to learn about the role of their genes of interest. Future experiments of *ccyA* heteroploidy mutants should be studied with SEM to observe their iACC granules and compare with the wildtype strain. This analysis could offer clues about the functional role of *ccyA* in intracellular biomineralization.

4.3 The IPTG-Inducible CRISPRi System in *Cyanothece* sp. PCC 7425 and Its Challenges

The CRISPRi experiments aiming to repress the control gene *nblA* in C.7425 did not yield a distinguishable phenotype when compared to the wildtype, in contrast to previous studies that showed a clear phenotype (color change) upon *nblA* repression in model cyanobacteria using CRISPRi, (Sun Young Choi & Han Min Woo 2020). As mentioned in section 3.3 of Results, analysis of CRISPRi repression of *ccyA* was not initiated due to this negative result of the control gene. The lack of phenotype could be due to several potential factors. C.7425 may exhibit different physiological responses during nitrogen starvation compared to the model strains. As a diazotrophic cyanobacterium capable of anaerobically fixing atmospheric nitrogen (Chenebault *et al*. 2020), its cellular state during oxic nitrogen starvation might differ from the non-diazotrophic model strains. This could potentially have an effect on *nblA* expression and therefore its CRISPRi-mediated repression. Hence, the repression experiment was also conducted in high-light stress instead of nitrogen deficiency stress, as high-light stress is a known condition for phycobilisome degradation (Sendersky *et al.* 2015). However, no difference between wildtype and mutants could be observed in this case as well. Another potential factor could be that the CRISPRi plasmid was incorrect. Only the insertions of the spacers into the CRISPR array were previously verified by PCR and sequencing. If the constructs are correct then the inefficiency of the CRISPRi system might stem from a limited diffusion or import rate of IPTG, the inducer of the dCas12a gene and the CRISPR array on

the plasmid pSL3287. It is not established whether C.7425 can actively transport lactose, and its analogues such as IPTG, into the cells. Therefore, the intracellular concentration of IPTG might not be significant enough to induce the CRISPRi system up to an observable phenotype. If true, one solution to this problem could be to introduce an active lactose permease into C.7425, for example by overexpression of *E. coli lacY* from a pC-plasmid. This solution has earlier been utilized in *Pseudomonas fluorescens* and increased inducibility five times at 0.1 mM IPTG (Hansen *et al.* 1998). Another factor might be the *trc*2O promoter on the pSL3287 plasmid, which controls the dCas12a expression, and has been noted for strong repression but low induction levels (Huang *et al.* 2010). Even addition of up to 10 mM IPTG did not increase expression significantly. Therefore, expression levels of the dCas12a might not be sufficient for repression of *nblA*, leading to a visible phenotype. To test for the expression of dCas12a from pSL3287 in C.7425, analyzing transcription levels using techniques such as RT-PCR could be a viable solution. However, if C.7425 is unable to import IPTG the promotor will not be induced either way. This might suggest the need to explore alternative promotors or induction systems for C.7425. The anhydrotetracycline (aTc) induction system was critical for achieving inducible repression with CRISPRi in *Synechococcus* sp. PCC 7002 and has been optimized for CRISPRi in *Synechocystis* sp. PCC 6803 (Gordon *et al*. 2016; Kiyan Shabestary *et al.* 2018). Although, aTc has been shown sensitive to light, with a decrease of the dynamic range of induction in *Synechococcus* sp. PCC 7002 after 24-48 hours of exposure (Zess *et al.* 2015).

Developing a successful CRISPRi system for to repress *ccyA* in C.7425 make possible physiological experiments under various growth conditions. Inducing repression of *ccyA* and analysing the resulting changes in $CaCO_3$ granule formation and biomineralization parameters such as pH and Ca^{2+} uptake could provide valuable insights into the role of *ccyA*.

5 Conclusion

This project aimed at investigating the function of CcyA in *Cyanothece* sp. PCC 7425 (C.7425) through overexpression, deletion and repression. Despite some challenges, valuable insights were gained and several promising pathways for future research were identified. The overexpression experiments of *ccyA* indicated a potential link between pH changes in growth media and Ca^{2+} uptake in C.7425. While it did not impact growth in standard or limiting Ca^{2+} conditions, it increased extracellular pH which is an indicator for extracellular biomineralization. The reason for Ca^{2+} release into the media following pH peaks will be studied.

The CRISPR/Cas12a system successfully facilitated the deletion of two *CAX* genes and *ccyA* in C.7425. However, for *ccyA* deletion a complete chromosome segregation was not achieved indicating that *ccyA* might be crucial for the growth of C.7425. Partially chromosome segregated mutants can still offer valuable information on *ccyA* and intracellular biomineralization. Future work should include SEM analyses to compare partially segregated mutants with wildtypes, verifying if there are any differences in the number and size of $CaCO_3$ inclusions. In conclusion, the CRISPR/Cas12a system used in this project for deletion with HDR was proven to work in C.7425, which has never been tried before.

The CRISPRi experiments aimed at repressing *nblA*, as a reporter gene for verifying that the CRISPRi system worked, did not produce a noticeable phenotype, likely due to physiological differences in C.7425 or limitations in the inducibility of the CRISPRi system. Future strategies should first include sequencing the plasmids to verify the constructs are correct. If correct, the next strategies could be enhancing IPTG import by overexpressing lactose permease and analysing expression levels of dCas12a or exploring alternative induction systems such as aTc.

6 Acknowledgement

I would like to first express my gratitude to my supervisor, Franck Chauvat, for giving me the opportunity to do my master's thesis project in the LBBC lab at CEA Paris-Saclay. His guidance and teaching have been essential, and I am honored by his belief in my ability to contribute to the project. I extend my heartfelt thanks to my co-supervisor, Monis Athar Khan, for all his support, for teaching me everything in the lab, and for always being there to answer my questions. A big thank you to Corinne Chauvat for her enthusiastic discussions about the project and for helping me with any problems I faced in the lab. Lastly for LBBC, I would like to thank everyone in the lab for welcoming me and letting me be a part of the team during my master's thesis. I would like to thank my subject reader, Pia Lindberg, for her insights, valuable feedback, and enthusiasm about my project.

References

Baldanta S, Guevara G, Navarro-Llorens JM. 2022. SEVA-Cpf1, a CRISPR-Cas12a vector for genome editing in cyanobacteria. Microbial Cell Factories, doi https://doi.org/10.1186/s12934-022-01830-4.

Bandyopadhyay A, Elvitigala T, Welsh E, Stöckel J, Liberton M, Min H, Sherman LA, Pakrasi HB. 2011. Novel Metabolic Attributes of the Genus Cyanothece , Comprising a Group of Unicellular Nitrogen-Fixing Cyanobacteria. mBio, doi https://doi.org/10.1128/mbio.00214-11.

Benzerara K, Duprat E, Tristan B-F, Caumes G, Cassier-Chauvat C, Chauvat F, Dezi M, Diop Seydina I, Geoffroy G, Görgen S, Muriel G, López-García P, Millet M, Skouri-Panet F, Moreira D, Isabelle C. 2022. A New Gene Family Diagnostic for Intracellular Biomineralization of Amorphous Ca Carbonates by Cyanobacteria. Genome Biology and Evolution, doi https://doi.org/10.1093/gbe/evac026.

Benzerara K, Skouri-Panet F, Li J, Férard C, Gugger M, Laurent T, Couradeau E, Ragon M, Cosmidis J, Menguy N, Margaret-Oliver I, Tavera R, López-García P, Moreira D. 2014. Intracellular Ca-carbonate biomineralization is widespread in cyanobacteria. Proceedings of the National Academy of Sciences 111: 10933–10938.

Berla BM, Saha R, Immethun CM, Maranas CD, Moon TS, Pakrasi HB. 2013. Synthetic biology of cyanobacteria: unique challenges and opportunities. Frontiers in Microbiology, doi https://doi.org/10.3389/fmicb.2013.00246.

Cam N, Benzerara K, Georgelin T, Jaber M, Lambert J-F, Poinsot M, Skouri-Panet F, Cordier L. 2016. Selective Uptake of Alkaline Earth Metals by Cyanobacteria Forming Intracellular Carbonates. Environmental Science & Technology 50: 11654–11662.

Cassier-Chauvat C, Blanc-Garin V, Chauvat F. 2021. Genetic, Genomics, and Responses to Stresses in Cyanobacteria: Biotechnological Implications. Genes 12: 500.

Chenebault C, Diaz-Santos E, Kammerscheit X, Görgen S, Ilioaia C, Streckaite S, Gall A, Robert B, Marcon E, Buisson D-A, Benzerara K, Sassi J-F, Cassier-Chauvat C,

Chauvat F. 2020. A Genetic Toolbox for the New Model Cyanobacterium Cyanothece PCC 7425: A Case Study for the Photosynthetic Production of Limonene. Frontiers in Microbiology, doi https://doi.org/10.3389/fmicb.2020.586601.

Couradeau E, Benzerara K, Gérard E, Moreira D, Bernard S, Brown GE, Purificación L-G. 2012. An Early-Branching Microbialite Cyanobacterium Forms Intracellular Carbonates. 336: 459–462.

De Wever A, Benzerara K, Coutaud M, Caumes G, Poinsot M, Skouri-Panet F, Laurent T, Duprat E, Gugger M. 2019. Evidence of high Ca uptake by cyanobacteria forming intracellular $CaCO_3$ and impact on their growth. Geobiology 17: 676–690.

Gaschignard G, Millet M, Bruley A, Benzerara K, Dezi M, Skouri-Panet F, Duprat E, Callebaut I. 2024. AlphaFold2-guided description of CoBaHMA, a novel family of bacterial domains within the heavy-metal-associated superfamily. Proteins, doi https://doi.org/10.1002/prot.26668.

Gordon GC, Korosh TC, Cameron JC, Markley AL, Begemann MB, Pfleger BF. 2016. CRISPR interference as a titratable, trans-acting regulatory tool for metabolic engineering in the cyanobacterium Synechococcus sp. strain PCC 7002. Metabolic Engineering 38: 170–179.

Görgen S, Benzerara K, Skouri-Panet F, Gugger M, Chauvat F, Cassier-Chauvat C. 2020. The diversity of molecular mechanisms of carbonate biomineralization by bacteria. Discover Materials, doi https://doi.org/10.1007/s43939-020-00001-9.

Han Z, Zhang Y, Zhao Y, Gao X, Tucker ME. 2022. Amorphous and Crystalline Carbonate Biomineralization in Cyanobacterial Biofilms Induced by *Synechocystis* sp. PCC6803 Cultured in $CaCl_2$–$MgCl_2$–$SrCl_2$ Mediums. Geomicrobiology journal 39: 767–780.

Hansen LH, Knudsen S, Sørensen SJ. 1998. The Effect of the lacY Gene on the Induction of IPTG Inducible Promoters, Studied in Escherichia coli and Pseudomonas fluorescens. Current Microbiology 36: 341–347.

Huang H-H, Camsund D, Lindblad P, Heidorn T. 2010. Design and characterization of molecular tools for a Synthetic Biology approach towards developing cyanobacterial biotechnology. Nucleic Acids Research 38: 2577–2593.

Jain A, Srivastava P. 2013. Broad host range plasmids. FEMS Microbiology Letters 348: 87–96.

Jiang H-B, Cheng H-M, Gao K-S, Qiu B-S. 2013. Inactivation of Ca2+/H+Exchanger in Synechocystis sp. Strain PCC 6803 Promotes Cyanobacterial Calcification by Upregulating CO2-Concentrating Mechanisms. Applied and Environmental Microbiology 79: 4048–4055.

Kasinak J-ME, Holt BM, Chislock MF, Wilson AE. 2014. Benchtop fluorometry of phycocyanin as a rapid approach for estimating cyanobacterial biovolume. Journal of Plankton Research 37: 248–257.

Kiyan Shabestary, Anfelt J, Ljungqvist E, Jahn M, Yao L, Hudson EP. 2018. Targeted Repression of Essential Genes To Arrest Growth and Increase Carbon Partitioning and Biofuel Titers in Cyanobacteria. ACS synthetic biology 7: 1669–1675.

Knoot CJ, Biswas S, Pakrasi HB. 2019. Tunable Repression of Key Photosynthetic Processes Using Cas12a CRISPR Interference in the Fast-Growing Cyanobacterium Synechococcus sp. UTEX 2973. ACS Synthetic Biology 9: 132–143.

Lamérand C, Shirokova LS, Bénézeth P, Rols J-L, Pokrovsky OS. 2022. Carbon sequestration potential of Mg carbonate and silicate biomineralization in the presence of cyanobacterium Synechococcus. Chemical geology 599: 120854–120854.

Li J, Margaret Oliver I, Cam N, Boudier T, Blondeau M, Leroy E, Cosmidis J, Skouri-Panet F, Guigner JM, Férard C, Poinsot M, Moreira D, Lopez-Garcia P, Cassier-Chauvat C, Chauvat F, Benzerara K. 2016. Biomineralization Patterns of Intracellular Carbonatogenesis in Cyanobacteria: Molecular Hypotheses. Minerals 6: 10–10.

McCutcheon J, Power IM, Shuster J, Harrison AL, Dipple GM, Southam G. 2019. Carbon Sequestration in Biogenic Magnesite and Other Magnesium Carbonate Minerals. Environmental Science & Technology 53: 3225–3237.

Mehta N, Benzerara K, Kocar BD, Chapon V. 2019. Sequestration of Radionuclides Radium-226 and Strontium-90 by Cyanobacteria Forming Intracellular Calcium Carbonates. Environmental Science & Technology 53: 12639–12647.

Mermet-Bouvier P, Chauvat F. 1994. A conditional expression vector for the cyanobacteriaSynechocystis sp. strains PCC6803 and PCC6714 orSynechococcus sp. strains PCC7942 and PCC6301. Current Microbiology 28: 145–148.

Moreira D, Tavera R, Benzerara K, Skouri-Panet F, Couradeau E, Gérard E, Loussert C, Novelo E, Zivanovic Y, López-García P. 2017. Description of Gloeomargarita lithophora gen. nov., sp. nov., a thylakoid-bearing, basal-branching cyanobacterium with intracellular carbonates, and proposal for Gloeomargaritales ord. nov. International Journal of Systematic and Evolutionary Microbiology 67: 653–658.

Niu T-C, Lin G-M, Xie L-R, Wang Z, Xing W-Y, Zhang J, Zhang C-C. 2019. Expanding the Potential of CRISPR-Cpf1-Based Genome Editing Technology in the Cyanobacterium *Anabaena* PCC 7120. 8: 170–180.

Powell B, Mergeay M, Christofi N. 1989. Transfer of broad host-range plasmids to sulphate-reducing bacteria. FEMS Microbiology Letters 59: 269–273.

Sendersky E, Kozer N, Levi M, Moizik M, Garini Y, Shav-Tal Y, Schwarz R. 2015. The proteolysis adaptor, NblA, is essential for degradation of the core pigment of the cyanobacterial light-harvesting complex. Plant journal 83: 845–852.

Sun Young Choi, Han Min Woo. 2020. CRISPRi-dCas12a: A dCas12a-Mediated CRISPR Interference for Repression of Multiple Genes and Metabolic Engineering in Cyanobacteria. ACS synthetic biology 9: 2351–2361.

Ungerer J, Pakrasi HB. 2016. Cpf1 Is A Versatile Tool for CRISPR Genome Editing Across Diverse Species of Cyanobacteria. Scientific Reports, doi https://doi.org/10.1038/srep39681.

Vavitsas K, Kugler A, Satta A, Hatzinikolaou DG, Lindblad P, Fewer DP, Lindberg P, Toivari M, Stensjö K. 2021. Doing synthetic biology with photosynthetic microorganisms. Physiologia Plantarum 173: 624–638.

Veaudor T, Blanc-Garin V, Chenebault C, Diaz-Santos E, Sassi J-F, Cassier-Chauvat C, Chauvat F. 2020. Recent Advances in the Photoautotrophic Metabolism of Cyanobacteria: Biotechnological Implications. Life 10: 71.

Veaudor T, Ortega-Ramos M, Jittawuttipoka T, Bottin H, Cassier-Chauvat C, Chauvat F. 2018. Overproduction of the cyanobacterial hydrogenase and selection of a mutant thriving on urea, as a possible step towards the future production of hydrogen coupled with water treatment. PloS one 13: e0198836–e0198836.

Wendt KE, Ungerer J, Cobb RE, Zhao H, Pakrasi HB. 2016. CRISPR/Cas9 mediated targeted mutagenesis of the fast growing cyanobacterium Synechococcus elongatus UTEX 2973. Microbial Cell Factories, doi https://doi.org/10.1186/s12934-016-0514-7.

Zess EK, Begemann MB, Pfleger BF. 2015. Construction of new synthetic biology tools for the control of gene expression in the cyanobacteriumSynechococcussp. strain PCC 7002. Biotechnology and Bioengineering 113: 424–432.

Appendix A - Chemical Composition of Culture Media

Supplementary table 1: Chemical Composition of Culture Media

Composition	**MM (mM)**	**MM-Ca (mM)**	**BG11 (mM)**	**BG11-Ca (mM)**
$NaNO_3$	17.65	17.65	17.65	17.65
K_2HPO_4	0.230	0.230	0.230	0.230
$MgSO_4.7H_2O$	0.304	0.304	0.304	0.304
$CaCl_2.2H_2O$	0.25	0	0.25	0
Citric Acid	0.031	0.031	0.031	0.031
Ferric Ammonium Citrate	0.022	0.022	0.022	0.022
IDRANAL	0.003	0.003	0.003	0.003
$NaHCO_3$	1.903	1.903	0.476	0.476
H_3BO_3	0.046	0.046	0.046	0.046
$MnCl_2.4H_2O$	0.009	0.009	0.009	0.009
$ZnSO_4.7H_2O$	0.0007	0.0007	0.0007	0.0007
$Na_2MoO_4.2H2O$	0.0019	0.0019	0.0019	0.0019

$CuSO_4.5H2O$	0.00049	0.00049	0.00049	0.00049
$Co(NO_3)_3.6H2O$	0.00027	0.00027	0.00027	0.00027
HEPES	2	2		

Appendix B - List of Strains and Plasmids

Supplementary table 2: List of strains and plasmids.

Strain/Plasmid	**Features**	**Reference**
	Escherichia coli	
Escherichia coli CM404	Helper strain used in triparental conjugation, harbours the self-transmissible RP4 plasmid.	Powell *et al.* (1989)
Escherichia coli NEB10-beta	DH10B derivative used for cloning and triparental conjugation of RSF1010 derivatives	New England Biolabs
	Cyanobacteria	
Cyanothece sp. PCC 7425	Unicellular, diazotrophic, photoautotrophic iACC forming strain with inclusions scattered throughout the cytoplasm	Pasteur Institute (Paris, France)
Synechococcus PCC 7942	Model unicellular photoautotrophic cyanobacterium.	Pasteur Institute (Paris, France)
pC	RSF1010 derivative plasmid harbouring strong λ phage pR promoter for constitutive expression. (Sm^R/Sp^R, Cm^{SR})	Veaudor *et al.* (2018)
$pC_{ccyAC7425}$	pC derivative plasmid harbouring the *ccyA*	Görgen unpublished

	sequence from *Cyanothece* sp. PCC 7425 cloned at *Nde*I and *EcoR*I sites. (Sm^R/Sp^R, Cm^S)	
$pC_{ccyAS6312}$	pC derivative plasmid harbouring the *ccyA* sequence from *Synechococcus* sp. PCC 6312 cloned at *Nde*I and *EcoR*I sites. (Sm^R/Sp^R, Cm^S)	Görgen unpublished
pC_{ccyAC7}	pC derivative plasmid harbouring the *ccyA* sequence from *Gloeomargarita lithophora* C7 cloned at *Nde*I and *EcoR*I sites. (Sm^R/Sp^R, Cm^S)	Görgen unpublished
pSL2680	RSF1010 derivative plasmid. Contains the Cas12a nuclease gene expressed from a Lac promoter and *Aar*I – *LacZα* – *Aar*I site for cloning of spacer sequences flanked by CRISPR repeats where *LacZα* is expressed from a Lac promotor and the CRISPR array from a J23119 constitutive promoter. (Km^R/Neo^R)	Ungerer and Pakrasi (2016) (Addgene plasmid # 85581 ; http://n2t.net/addgene:85581 ; RRID:Addgene_85581)
p$\Delta ccyA_{C7425}$crRNA1	pSL2680 derivative plasmid. Harbouring spacer sequence 1 in the CRISPR array for	This study

	ccyA of *Cyanothece* sp. PCC 7425 cloned at *Aar*I and ~500 bp upstream and downstream homology platforms with a Sm^R/Sp^R cassette in-between cloned at *Sal*I. (Km^R/Neo^R, Sm^R/Sp^R)	
p$\Delta ccyA_{C7425}$crRNA2	pSL2680 derivative plasmid. Harbouring spacer sequence 2 in the CRISPR array for *ccyA* of *Cyanothece* sp. PCC 7425 cloned at *Aar*I and ~500 bp upstream and downstream homology platforms with a Sm^R/Sp^R cassette in-between cloned at *Sal*I. (Km^R/Neo^R, Sm^R/Sp^R)	This study
pΔCAX_{C7425}crRNA1	pSL2680 derivative plasmid. Harbouring spacer sequence 1 in the CRISPR array for *CAX3000* of *Cyanothece* sp. PCC 7425 cloned at *Aar*I and ~400-600 bp upstream and downstream homology platforms with a Sm^R/Sp^R cassette in-between cloned at *Sal*I. (Km^R/Neo^R, Sm^R/Sp^R)	This study
pΔCAX_{C7425}crRNA2	pSL2680 derivative plasmid. Harbouring spacer sequence 2 in the CRISPR array for *CAX3001* of *Cyanothece* sp. PCC 7425 cloned at *Aar*I and ~400-600 bp upstream and downstream homology platforms with a Sm^R/Sp^R	This study

	cassette in-between cloned at *Sal*I. (Km^R/Neo^R, Sm^R/Sp^R)	
pSL3287	RSF1010 derivative plasmid. Harbouring a dCas12a gene under control of a *trc2O* promoter and *Aar*I – *LacZα* – *Aar*I site for cloning of spacer sequences flanked by CRISPR repeats where *LacZα* is expressed from a Lac promotor and the CRISPR array is under control of a *lac1O* promotor. For repression of lac operators, it harbours the *lacI* mutant *W220F* expressed from a J23119 constitutive promoter. (Km^R/Neo^R)	Knoot *et al.* (2019) (Addgene plasmid # 139750 ; http://n2t.net/addgene:139750 ; RRID:Addgene_139750)
pSL3287$_{ccyAC7425}$crRNA3	pSL3287 derivative plasmid. Harbouring spacer sequence 3 in the CRISPR array for repression of *ccyA* in C.7425, cloned at *AarI* site. (Km^R/Neo^R)	This study
pSL3287$_{ccyAC7425}$crRNA3-crRNA4	pSL3287 derivative plasmid. Harbouring spacer sequence 4 in the CRISPR array, for repression of *ccyA* in *Cyanothece* sp. PCC 7425, cloned at *AarI* site. (Km^R/Neo^R)	This study
pSL3287$_{nblA0220C7425}$crRNA1	pSL3287 derivative plasmid. Harbouring spacer sequence	This study

	1 in the CRISPR array, for repression of *nblA0220* in C.7425, cloned at *AarI* site. (Km^R/Neo^R)	
pSL3287$_{nblAC7425}$crRNA1-crRNA2	pSL3287 derivative plasmid. Harbouring spacer sequence 1 and 2 for repression of *nbla0220* and *nblA2827* in C.7425, cloned at *AarI* site. (Km^R/Neo^R)	This study

Appendix C - List of Primers and their Sequences

Supplementary table 3: List of primers and their sequences.

Name	**Sequence (5' to 3')**	**Aim**	**Localization of primer**	**PCR program**
C7425-ccyA-Spacer1-Fw	agatCAGGAATTGACCTTGCGCCACG	Annealing of spacer for insertion to CRISPR array	400 bp downstream of transcription start site of *ccyA* on C7425 chromosome.	95 °C for five minutes and then cooled to 4 °C with a rate of 0,1 °C per second
C7425-ccyA-Spacer1-Rv	agacCGTGGCGCAAGGTCAATTCCTG			
C7425-ccyA-Spacer2-Fw	agatCCTGCAACAACAAATTCAATCC		150 bp downstream of transcription start site of *ccyA* on C7425 chromosome.	
C7425-ccyA-Spacer2-Rv	agacGGATTGAATTTGTTGTTGCAGG			
C7425-ccyA-Spacer3-Fw	agacCTGATCCATGCTATTACCGGAC		75 bp downstream of transcription start site of *ccyA* on C7425 chromosome.	
C7425-ccyA-Spacer3-Rv	agatGTCCGGTAATAGCATGGATCAG			
C7425-ccyA-Spacer3-Spacer4-Fw	agacTCTCTGCCTATCTGTTGATCTGatctacaacagtagaaattatttaaagttcttagacCTGATCCATGCTATTACCGGAC		Spacer 3 is 75 bp downstream of transcription start site and Spacer 4 is 60 bp upstream of transcription start site *ccyA* on	

	Red = Repeat sequence of CRISPR array		C7425 chromosome.	
C7425-ccyA-Spacer3-Spacer4-Rv	agatGTCCGGTAATAGCATGGATCAGgtctaagaacttaaataatttctactgttgtagatCAGATCAACAGATAGGCAGAGA Red = Repeat sequence of CRISPR array			
C7425-CAX-Spacer1-Fw	agatATTGGTTCCATTATTGCCAACC		Spacer 1 is 282 bp downstream of transcription start site of *CAX3000* on C7425 chromosome.	
C7425-CAX-Spacer1-Rv	agacGGTTGGCAATAATGGAACCAAT			
C7425-CAX-Spacer1-Spacer2-Fw	agatATTGGTTCCATTATTGCCAACCatctacaacagtagaaattatttaaagttcttagacGAAAAAGCCATTGCTAGCGTGG Red = Repeat sequence of CRISPR array		Spacer 1 is 282 bp downstream of transcription start site of *CAX3000* and Spacer 2 is 702 bp upstream of transcription start site of *CAX3001* on C7425 chromosome.	
C7425-CAX-Spacer1-Spacer2-Rv	agacCCACGCTAGCAATGGCTTTTTCgtctaagaacttaaataatttctactgttgtagatGGTTGGCA			

	ATAATGGAACCAAT Red = Repeat sequence of CRISPR array			
C7425-nblA-Spacer1-Fw	agacAACAACAATTCCAGATGCGTTT		Spacer 1 is 43 bp downstream of transcription start site of *nblA0220* on C7425 chromosome.	
C7425-nblA-Spacer1-Rv	agatAAACGCATCTGGAATTGTTGTT			
C7425-nblA-Spacer1-Spacer2-Fw	agacAACAACAATTCCAGATGCGTTTatctacaacagtagaaattatttaaagttcttagacAGTTACAAGTTATTGAAAGTGA Red = Repeat sequence of CRISPR array		Spacer 1 is 43 bp downstream of transcription start site of *nblA0220* and Spacer 2 is 46 bp downstream of transcription start site of *nblA2827* on C7425 chromosome.	
C7425-nblA-Spacer1-Spacer2-Rv	agatTCACTTTCAATAACTTGTAACTgtctaagaacttttaaataatttctactgttgtagatAAACGCATCTGGAATTGTTGTT Red = Repeat sequence of CRISPR array			
G-7425-ΔccyA-Fw	agctttaatgcggtagttggtaccgtcgacCCA	Amplifying the Sm^R/Sp^R cassette flanked by homology	Has an homology overhang upstream of *Sal*I site on pSL2680	Hybridization temperature – 62,5 °C

	GTCACGACGTTGTAAAAC Blue = Overlapping regions for Gibson assembly	platforms as homology directed repair template and cloning it into pSL2680 at *Sal*I by Gibson assembly.	and binds upstream of the homology directed repair template on an in-house pTwist plasmid.	Extension time – 4 min 42s
G-7425-ΔccyA-Rv	tgcccggattacagatcctctagagtcgacTTCACACAGGAAACAGCTATGACCAT Blue = Overlapping regions for Gibson assembly		Has an homology overhang downstream of *Sal*I site on pSL2680 and binds downstream of the homology directed repair template on an in-house pTwist plasmid.	
G-7425-ΔCAX-UP-Fw	agctttaatgcggtagttggtaccgtcgacTGCCACCGACATTGCCCGA Blue = Overlapping regions for Gibson assembly	Recovering an upstream region of *CAX3000* from C7425 chromosome as homology platform for cloning into pSL2680 by Gibson assembly.	Has an homology overhang for upstream of *Sal*I site on pSL2680 and binds to start of upstream region of *CAX3000* in C7425.	Hybridization temperature – 64,4 °C Extension time – 1min 18s
G-7425-ΔCAX-UP-Rv	gcgtgagcgcataGATTGCCTCTGAACGGTTCCG Blue = Overlapping regions for Gibson assembly		Binding to end of upstream region of *CAX3000* on C7425 and has homology overhang upstream of Sm^R/Sp^R cassette.	

G-7425-ΔCAX-SmRSpR-Fw	tcagaggcaatcTATGCGCTCACGCAACTGG Blue = Overlapping regions for Gibson assembly	Recovering Sm^R/Sp^R cassette platform from pC plasmid for cloning into pSL2680 by Gibson assembly. To be flanked by upstream and downstream homology platforms.	Binding to start of Sm^R/Sp^R region of pC plasmid and has homology overhand for end of upstream homology platform.	Hybridization temperature – 59,4 °C Extension time – 2min 10s
G-7425-ΔCAX-SmRSpR-Rv	ccggatttgatccGGCGTCGGCTTGAACG Blue = Overlapping regions for Gibson assembly		Binding to end of Sm^R/Sp^R region of pC plasmid and has homology overhang for start of downstream homology platform.	
G-7425-ΔCAX-DOWN-Fw	caagccgacgccGGATCAAATCCGGTCAGGATGGGGAAT Blue = Overlapping regions for Gibson assembly	Recovering a downstream region of *CAX3001* in C.7425 as downstream homology platform for cloning into pSL2680 by Gibson assembly.	Binding to start of downstream homology platform and has a homology overhang downstream on Sm^R/Sp^R cassette.	Hybridization temperature – 66,1 °C Extension time – 1min 18s
G-7425-ΔCAX-DOWN-Rv	tgcccggattacagatcctctagagtcgacCTTCCCTGGGGGGACCGA Blue = Overlapping regions for Gibson assembly		Binding to end of downstream homology platform and has a homology overhang for the pSL2680 plasmid downstream of *Sal*I.	

crRNAseq-Fw	TCTTGACAGCTAGCTCAGTCC	Verification of CRISPR-array insert on pSL2680 derivatives.	Binds to start of the J23119 promoter.	Hybridization temperature – 57.7 °C Extension time for all pSL2680 derivatives: 30s
crRNAseq-Rv	GACCGGCTACTAATACAAAAGG		Binds downstream of *Aar*I site in CRISPR array.	
crRNA-platforms-Rv	GCCCGGATTACAGATCCTCT	Verification of insert of CRISPR array and homology directed repair template on pSL2680. Used with primer crRNAseq-Fw.	Binds downstream of *Sal*I site.	Hybridization temperature – 58.3 °C Extension time for all pSL2680 derivates – 2min 45s
crRNAseq2-Fw	GACCGGCTACTAATACAAAAGG	Verification of CRISPR array on pSL3287.	Bind upstream of *Aar*I site in the CRISPR array.	Hybridization temperature – 56.1 °C Extension time: pSL3287$_{ccyAC7425}$crRNA3 – 2min 18s pSL3287$_{nblA0220C7425}$crRNA1 – 2min 18s pSL3287$_{ccyAC7425}$crRNA3-crRNA4 – 2min 24s
crRNAseq2-Rv	GCCGCGATTAAATTCCAACA		Bind at the end of the Km^R/Neo^R cassette downstream of the CRISPR array.	

				pSL3287$_{nblAC7425}$crRNA1-crRNA2 – 2min 24s
ccyA-OU-Fw	ACAACACGTCAATCAATTCG	Verification of deletion with HDR of *ccyA* on C.7425 chromosome.	Upstream of the upstream homology platform "UP" on the chromosome.	Hybridization temperature – 53,6 °C Extension time – 4min 50s
ccyA-DO-Rv	TGGAGTCTGAACAGTTGACC		Downstream of the downstream homology platform "DOWN" on the chromosome.	
Omega_Fw	GATTTGCTGGTTACGGTGAC	Verification of Sm^R/Sp^R cassette.	Start of Sm^R/Sp^R cassette.	Hybridization temperature – 56,2 °C Extension time – 1min 20s
Omega_Rv	CCGACTACCTTGGTGATCTC		End of Sm^R/Sp^R cassette.	
CAX-OU-Fw	ATTAATGACTCTGCCGCCCT	Verification of deletion with HDR of *CAX* genes *CAX3000* and *CAX3001* on C.7425 chromosome.	Upstream of the upstream homology platform "UP" on the chromosome.	Hybridization temperature – 57,6 °C Extension time – 8 min
CAX-OD-Rv	ATCTGGGCACGTTACGGTTA		Downstream of the downstream homology platform "DOWN" on the chromosome.	

Appendix D - PCR Reaction Setup

Supplementary table 4: PCR reaction setup.

Component	**Volume of component for 25 µL**
H_2O	Add to 25 µL
10X DreamTaq™ Buffer	2.5 µL
10 µM Forward Primer	1 µL
10 µM Reverse Primer	1 µL
10 mM dNTPs	0.5 µL
DreamTaq™ DNA Polymerase	0.1 µL
Template DNA	1 or 5 µL*

*1 µL volume for DNA from Miniprep isolation using NucleoSpin® Plasmid EasyPure kit and 5 µL else and a sample plucked from a colony counts as 0 µL volume.

Appendix E - PCR Program

Supplementary table 5: PCR program for using DreamTaq™ DNA polymerase.

Cycle step	**Temperature**	**Time**	**Number of cycles**
Initial Denaturation*	98°C	30s	1
Denaturation	98°C	10s	25
Hybridization	X°C	30s	
Extension	72°C	Ys	
Final Extension	72°C	10min	1
Hold	4°C	∞	

X stands for hybridization temperature specific to primer pair and Y for extension time specific to length of region amplified (1 min per kb), see supplementary table 3 for values.

*For colony PCR the initial denaturation temperature is 94°C for 5 minutes for *E. coli* colonies and 10 minutes for cyanobacteria colonies.

Appendix F - Sampling Protocol for Growth Experiment with *ccyA* Overexpression Mutants

1. Weight each flask with culture separately.
2. Incubate for 48 hours or 72 hours if over the weekend.
3. Weight each flask with culture separately.
4. Add nuclease-free sterile H_2O to a volume that is based on the loss of weight due to the media evaporating during incubation.
5. Swirl the flask to mix.
6. Take a three mL sample.
7. Repeat from step 1.